JOURNAL OF PETROLOGY | VOLUME 47 | NUMBER 9 | PAGES 1673–1704 | 2006 | doi:10.1093/petrology/egl024

The Origin of HIMU in the SW Pacific: Evidence from Intraplate Volcanism in Southern New Zealand and Subantarctic Islands

K. S. PANTER[1]*, J. BLUSZTAJN[2], S. R. HART[2], P. R. KYLE[3], R. ESSER[3] AND W. C. McINTOSH[3]

[1]DEPARTMENT OF GEOLOGY, BOWLING GREEN STATE UNIVERSITY, BOWLING GREEN, OH 43403, USA

[2]DEPARTMENT OF GEOLOGY & GEOPHYSICS, WOODS HOLE OCEANOGRAPHIC INSTITUTION, WOODS HOLE, MA 02543, USA

[3]DEPARTMENT OF EARTH & ENVIRONMENTAL SCIENCE, NEW MEXICO INSTITUTE OF MINING & TECHNOLOGY, SOCORRO, NM 87801, USA

RECEIVED JULY 28, 2005; ACCEPTED MARCH 29, 2006; ADVANCE ACCESS PUBLICATION MAY 4, 2006

This paper presents field, geochemical and isotopic (Sr, Nd, Pb) results on basalts from the Antipodes, Campbell and Chatham Islands, New Zealand. New $^{40}Ar/^{39}Ar$ age determinations along with previous K–Ar dates reveal three major episodes of volcanic activity on Chatham Island (85–82, 41–35, ~5 Ma). Chatham and Antipodes samples comprise basanite, alkali and transitional basalts that have HIMU-like isotopic ($^{206}Pb/^{204}Pb$ > 20·3–20·8, $^{87}Sr/^{86}Sr$ <0·7033, $^{143}Nd/^{144}Nd$ >0·5128) and trace element affinities (Ce/Pb 28–36, Nb/U 34–66, Ba/Nb 4–7). The geochemistry of transitional to Q*-normative samples from Campbell Island is explained by interaction with continental crust. The volcanism is part of a long-lived (~100 Myr), low-volume, diffuse alkaline magmatic province that includes deposits on the North and South Islands of New Zealand as well as portions of West Antarctica and SE Australia. All of these continental areas were juxtaposed on the eastern margin of Gondwanaland at >83 Ma. A ubiquitous feature of mafic alkaline rocks from this region is their depletion in K and Pb relative to other highly incompatible elements when normalized to primitive mantle values. The inversion of trace element data indicates enriched mantle sources that contain variable proportions of hydrous minerals. We propose that the mantle sources represent continental lithosphere that host amphibole/phlogopite-rich veins formed by plume- and/or subduction-related metasomatism between 500 and 100 Ma. The strong HIMU signature ($^{206}Pb/^{204}Pb$ >20·5) is considered to be an in-grown feature generated by partial dehydration and loss of hydrophile elements (Pb, Rb, K) relative to more magmaphile elements (Th, U, Sr) during short-term storage at the base of the lithosphere.*

KEY WORDS: *continental alkaline basalts; lithospheric mantle, mantle metasomatism; New Zealand; OIB, HIMU; Sr, Nd and Pb isotopes; West Antarctica*

INTRODUCTION

It is widely accepted that most mafic alkaline magmas erupted in continental areas that have HIMU (high time-integrated $^{238}U/^{204}Pb$ or high μ) isotopic signatures similar to oceanic island basalts (OIB: $^{206}Pb/^{204}Pb$ >20·5 and low $^{87}Sr/^{86}Sr$ <0·7030 and $^{3}He/^{4}He$ 5–7 R/R_a) are products of small-degree melts from sub-lithospheric mantle sources (Wilson *et al.*, 1995; Ballentine *et al.*, 1997; Franz *et al.*, 1999; Janney *et al.*, 2002). The origin of the HIMU source component is often attributed to chemically modified oceanic lithosphere that was subducted and stored in the deep mantle, aged and eventually transported back to the surface via mantle plumes

*Corresponding author. Telephone: (1) 419-372-7337. Fax: (1) 419-372-7205. E-mail: kpanter@bgsu.edu

(Hofmann, 1997; Moreira & Kurz, 1999; Stracke *et al.*, 2003, 2005). However, it is becoming increasingly recognized that HIMU sources may also exist within sub-continental lithosphere, generated by the infiltration of metasomatic fluids and melts (Stein *et al.*, 1997; Blusztajn & Hegner, 2002; Pilet *et al.*, 2005). A lithospheric versus sub-lithospheric origin of the HIMU component in continental basalts in the SW Pacific (New Zealand, West Antarctica and SE Australia) has been a matter of debate for several decades.

The intraplate igneous rocks of southern New Zealand are low in volume ($<10\,000\,km^3$), widely scattered within a 1000 km × 800 km area and include several large shield volcanoes, mafic lava fields and small intrusive complexes (Weaver & Smith, 1989). The mafic rocks are predominantly alkaline and have OIB-like major and trace element compositions and isotopic signatures that resemble a HIMU mantle source (Gamble *et al.*, 1986; Barreiro & Cooper, 1987; Weaver & Smith, 1989; Baker *et al.*, 1994; Hoke *et al.*, 2000). Coombs *et al.* (1986) and Sun *et al.* (1989) recognized the regional OIB–HIMU like character of continental volcanism in New Zealand, Tasmania and West Antarctica. Lanyon *et al.* (1993), Weaver *et al.* (1994) and Storey *et al.* (1999) related the HIMU volcanism to mantle plume sources that entered the upper mantle beneath Gondwanaland in the mid- to late Cretaceous and suggested that plume activity played a role in Antarctic–New Zealand break-up and the opening of the Tasman Sea. A younger and smaller plume has been invoked to explain Cenozoic uplift and volcanism in Marie Byrd Land (LeMasurier & Rex, 1989; Behrendt *et al.*, 1992, 1996; Hole & LeMasurier, 1994; LeMasurier & Landis, 1996; Storey *et al.*, 1999). An alternative plume model is one in which the source for all of the HIMU volcanism in the SW Pacific can be related to an ancient plume head that was fossilized in the uppermost mantle prior to Gondwanaland break-up (Rocholl *et al.*, 1995; Hart *et al.*, 1997; Panter *et al.*, 2000*a*). Others have proposed magmatism without plume origins. Rocchi *et al.* (2002, 2004) suggested that the upper mantle source for the alkaline magmas was metasomatically enriched during late Cretaceous extension and subsequently melted in response to reactivation of trans-lithospheric fractures during Cenozoic times. Finn *et al.* (2005) proposed that the Cenozoic volcanism forming this Diffuse Alkaline Magmatic Province (DAMP) is a response to the sudden detachment and sinking of subducted slabs into the lower mantle causing vertical and lateral flow that triggered melting of a previously metasomatized mantle lithosphere.

Past studies are weighted heavily on data gathered from Cenozoic basalts but most of the models call upon sources that are at least Mesozoic in age. Prior to this study, Mesozoic igneous rocks that approach OIB–HIMU end-member compositions in terms of Pb isotopes ($^{206}Pb/^{204}Pb > 20$) have been identified only within the mid-Cretaceous (*c.* 90–100 Ma) Tapuaenuku Igneous Complex (Baker *et al.*, 1994) on the South Island of New Zealand (Fig. 1). Other late Cretaceous continental basalts in New Zealand and Australia have similar geochemical characteristics but complete datasets, in particular Pb isotopes, are not yet published. We present here a detailed study of continental basalts from three islands off the east and southeastern coast of New Zealand (Fig. 1). The oldest basalts on Chatham Island are of late Cretaceous age (~85 Ma) with initial $^{206}Pb/^{204}Pb$ values ≥20 and trace element characteristics similar to OIB. The Cenozoic basalts from the same region, as well as basalts from Marie Byrd Land, West Antarctica (Hart *et al.*, 1997; Panter *et al.*, 2000*a*) have very similar isotopic and trace element characteristics. The purpose of this study is to: (1) constrain the processes involved in the genesis of mafic magmas in southern New Zealand; (2) determine mantle source compositions; (3) evaluate the origin of the HIMU-like signature; (4) use the new data to help constrain regional models proposed for the magmatism.

REGIONAL GEOLOGICAL HISTORY

The Campbell and Antipodes islands are situated along the southeastern margin of the submarine Campbell Plateau, whereas the Chatham Islands lie at the eastern end of the Chatham Rise (Fig. 1). The basement geology of the Chatham Rise and Campbell Plateau consists of Paleozoic–Mesozoic metasedimentary and plutonic rocks (Beggs *et al.*, 1990; Wood & Herzer, 1993) that correlate with major tectonostratigraphic terranes recognized on the mainland of New Zealand (Bishop *et al.*, 1985; Bradshaw, 1989; Adams *et al.*, 1998) and in Marie Byrd Land, Antarctica (Bradshaw *et al.*, 1997; Pankhurst *et al.*, 1998; Sutherland, 1999).

The late Cretaceous break-up of the proto-Pacific margin of Gondwanaland was foreshadowed by mid-Cretaceous extension and crustal thinning over a broad area (Bradshaw, 1989; Beggs, 1993; Davy, 1993; Laird, 1993; Luyendyk *et al.*, 2001, 2003), rapid regional uplift (Tulloch & Kimbrough, 1989; Richard *et al.*, 1994; Adams *et al.*, 1995; Spell *et al.*, 2000) and a sudden change from subduction-related to extension-related magmatism (Weaver *et al.*, 1994; Tulloch & Kimbrough, 1995; Waight *et al.*, 1998*a*). The switch in tectonic regime corresponded to the oblique arrival of the Pacific–Phoenix spreading center along the Gondwanaland margin at ~100 Ma (Bradshaw, 1989; Luyendyk, 1995; Mukasa & Dalziel, 2000). Ultimately, the interaction between the Pacific–Phoenix spreading center and the subduction zone led to the break-up of the supercontinent and inception of the Pacific–Antarctic Ridge shortly before 83 Ma (Molnar *et al.*, 1975; Larter *et al.*, 2002).

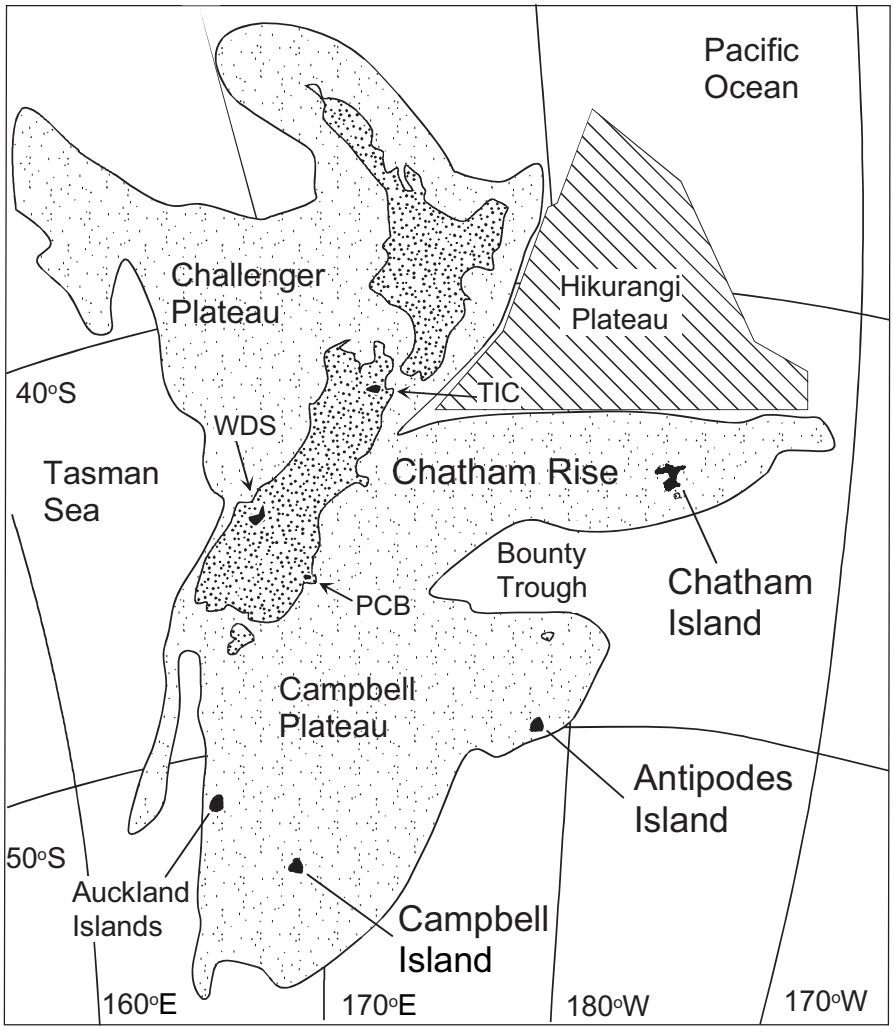

Fig. 1. Regional location map of New Zealand showing the location of Campbell, Antipodes and Chatham Islands. The Challenger Plateau, Campbell Plateau and Chatham Rise are areas of submerged continental crust. The Hikurangi Plateau is a large oceanic plateau. Also shown are locations for the Westland dike swarm (WDS), Tapuaenuku Igneous Complex (TIC) and Port Chalmers Breccia (PCB).

Cretaceous extension-related magmatism along the New Zealand sector of the Gondwanaland margin includes the Mandamus (Weaver & Pankhurst, 1991), Tapuaenuku (Baker *et al.*, 1994) and Blue Mountain (Grapes, 1975) layered igneous complexes, numerous other intrusions (Waight *et al.*, 1998*b*) and dispersed volcanic fields, including a large basaltic shield volcano on the Chatham Islands (Grindley *et al.*, 1977). These igneous rocks range in age from 100 to 60 Ma with a peak in activity between 100 and 90 Ma (Baker *et al.*, 1994; Table 1). Following continental break-up, New Zealand experienced pronounced thermal relaxation as it moved northward on the Pacific Plate. Consequently, the Paleocene–Eocene epochs were a period of relative magmatic quiescence (Weaver & Smith, 1989) and volcanic rocks of late Eocene to early Oligocene age are minor in volume and widely dispersed.

Over the past 45 Myr tectonic activity in New Zealand has been the result of the progressive development of the Australian–Pacific plate boundary (Sutherland, 1995). Transtension and inception of the paleo-Alpine Fault system, whose age is constrained by dikes of the Westland swarm (Fig. 1) emplaced between 32 and 25 Ma (Adams & Cooper, 1996), was followed by transpression and rapid uplift of the Southern Alps beginning at ~6 Ma (Walcott, 1998). Adams & Cooper (1996) proposed that the termination of a major volcanic episode, which produced several large igneous centers on the Banks and Dunedin Peninsulas in the middle to late Miocene, was a response to the change to a compressive tectonic regime.

Pliocene–Pleistocene volcanism in southern New Zealand was restricted to small areas on the South Island (Duggan & Reay, 1986) and on Antipodes and Chatham

Table 1: Summary of petrographic characteristics of porphyritic samples from Campbell and Chatham Islands, New Zealand

Sample	Location	Deposit type	Rock type	Age/unit	Phenocrysts				Texture
					>5%	<5%	Other	% Total	
OU36163	Campbell Is.	lava	subalk	~7	pl	ol>cpx	mt	24	p, hc, tc
OU36173	Campbell Is.	lava	trans bas	~7	pl	cpx>ol	mt	21	p, hc, tc
OU39771	Campbell Is.	dike	trans bas	~7	pl	cpx	mt	13	p, hc
Chatham Island									
CHT-1	Ohira Bay	lava	akb	ps	—	ol>cpx	mt	2	fp, hc, tc
CHT-3	Ohira Bay Quarry	lava	akb	ps	—	ol>cpx	mt	2	fp, hc
CHT-4	Owenga Rd.	lava	basalt	ps	—	ol~cpx>pl	mt	1	mp, hphy, amg
CHT-5	Cape Young	lava	basanite	mr	ol	cpx~amp	mt	11	p, hpc, amg
CHT-8	Cape Young	lava	basanite	mr	cpx>amp	ol	mt	13	p, hpc, amg
CHT-9	Mairangi	block	trans bas	kn	ol	cpx	—	7	mp, hpc, tc
CHT-10	Mt. Chudleigh	plug	basanite	kn	—	ol>cpx	mt	5	hphy
CHT-11	Mt. Chudleigh	lava	basanite	kn	ol	cpx	—	6	fp, hpc
CHT-12	Waitaha Creek	lava	trans bas	ps	—	ol~cpx	mt	8	mp, hc
CHT-14	Korako Hill	block	BTA	kn	pl>cpx	ol	mt	26	mp, vtph, amg
CHT-15	Matakitaki	tuff	basalt	kn	ol~cpx	—	mt	15	vtph, palg
CHT-16	Maunganui	lava	tephrite	mr	—	ol	—	1	hphy
CHT-17	Maunganui	lava	tephrite	mr	—	ol>cpx>amp	mt	6	fp, hpc, v
CHT-18	West Rd. Quarry	lava	akb	kn	—	cpx>ol	—	7	fp, hpc, v
CHT-19	Tawreikoko	dike	basalt	mr	—	cpx>ol>pl	mt	6	hpc, v, amg
CHT-20	Tawreikoko	dike	basanite	mr	ol~cpx	amp	mt	20	p, hpc, amg
CHT-21	Tuku River	lava	trans bas	ps	ol~cpx	pl	mt	13	fp, hc
CHT-22	Tuku River	lava	trans bas	ps	—	ol>cpx	mt	7	fp, hc, tc
CHT-23	Tuku River	lava	trans bas	ps	ol	cpx	—	10	fp, hc
CHT-24	Tuku River	lava	trans bas	ps	cpx>ol	—	mt	12	fp, hc
CHT-25	Tuku River	lava	trans bas	ps	cpx>ol	pl	mt	14	fp, hc, tc
CHT-26	Tuku River	lava	trans bas	ps	—	cpx>ol>pl	mt	5	fp, hc
CHT-27	Cape Fournier	lava	trans bas	ps	cpx>ol	—	mt	11	fp, hc

ps, late Cretaceous Southern Volcanics; kn, Eocene Northern Volcanics; mr, Pliocene Rangitihi Volcanics; akb, alkali basalt; BTA, basaltic trachyandesite; trans bas, transitional basalt; subalk, subalkali basalt. Phenocrysts: pl, plagioclase; ol, olivine; cpx, clinopyroxene; amp, amphibole; mt, magnetite. Texture: p, porphyritic; fp, finely porphyritic (phenocrysts <5 mm); mp, microporphyritic; v, vesicular (>10%); amg, amygdaloidal; hc, holocrystalline; hpc, hypocrystalline; hphy, hypohyaline; vtph, vitrophyric; palg, palagonitized; tc, trachytic.

Islands (Cullen, 1969; Grindley *et al.*, 1977). Although at present there is no active volcanism in southern New Zealand, geophysical evidence and helium emission studies indicate the existence of hot regions of decompressing upper mantle (Hoke *et al.*, 2000; Godfrey *et al.*, 2001).

VOLCANIC GEOLOGY

Campbell Island is New Zealand's southernmost subantarctic island (Fig. 1). Miocene volcanic rocks cover most of the island and consist of lava flows, pyroclastic rocks and volcanoclastic breccias (Morris, 1984; Morris & Gamble, 1990). Apart from a shallow intrusion of gabbro that predates volcanism by ~9 Myr, most of the deposits are late Miocene in age (~7·0 Ma, Adams *et al.*, 1979).

The Antipodes Islands are a small isolated island group that lies at the eastern edge of the Campbell Plateau (Fig. 1). The islands are composed of alkaline lavas and pyroclastic rocks, including tuff cone and ring deposits (Cullen, 1969; Gamble *et al.*, 1986; Gamble & Adams, 1990). A Quaternary age for the islands is inferred based on the well-preserved volcanic morphology and two K–Ar dates (Cullen, 1969).

The Chatham Islands are a populated group of islands that lie over 700 km east of the mainland of New Zealand (Fig. 1). The group consists of two main islands, Chatham

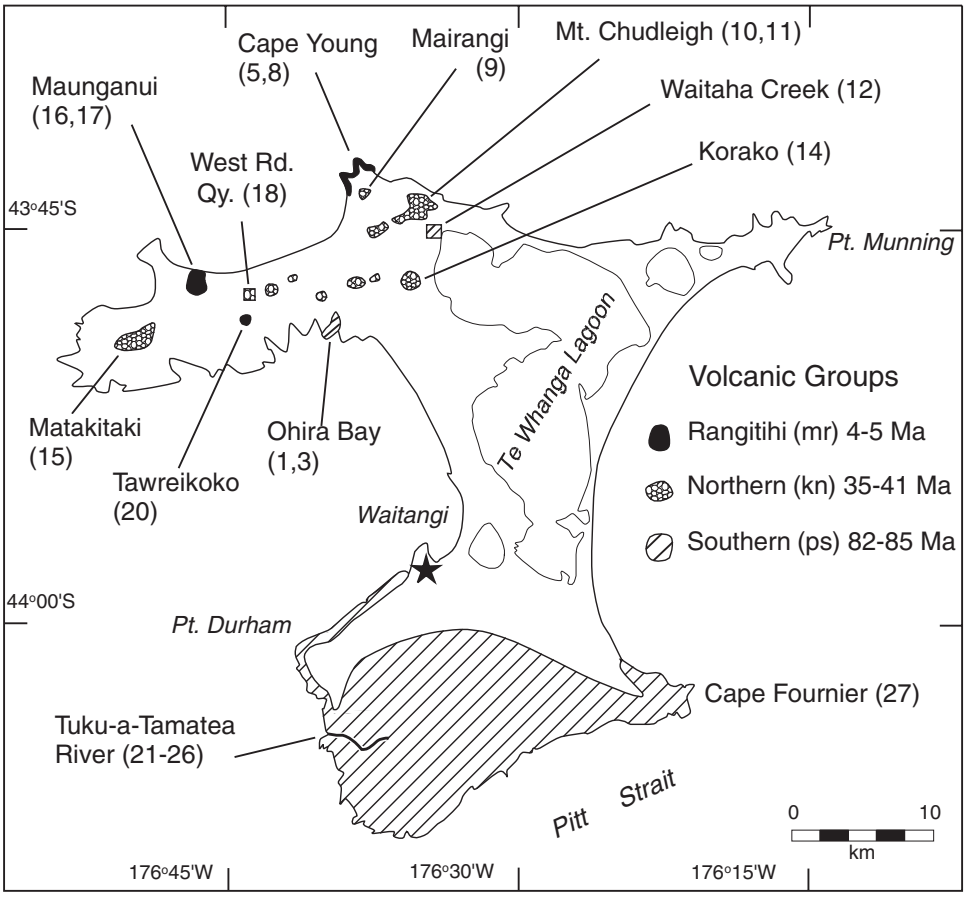

Fig. 2. Simplified geological map of Chatham Island showing exposures of the three major volcanic groups; late Cretaceous Southern Volcanics (ps), Eocene–Oligocene Northern Volcanics (kn) and Miocene–Pliocene Rangitihi Volcanics (mr) (Campbell *et al.*, 1993). The numbers in parenthesis that follow geographical names refer to samples collected [e.g. Matakitaki (15) is the location site of sample CHT-15].

and Pitt, which are surrounded by several smaller islands and a number of islet clusters. Campbell *et al.* (1993) provided a comprehensive review of the geology, geochronology and biostratigraphy of the Chatham Islands. The petrology and geochemistry of the Eocene and Cretaceous volcanic rocks have been reported by Morris (1985*a*, 1985*b*).

The mid- to late Cretaceous volcanic and sedimentary rocks of the Chatham Islands rest unconformably on a pre-Cretaceous basement of metasediments. The Cenozoic sequence consists of thin biogenic and clastic sedimentary units interspersed with localized volcanic deposits. Based on mapping and 26 K–Ar dates, Grindley *et al.* (1977) recognized that volcanism on the Chatham Islands occurred in three distinct episodes; late Cretaceous (81–70 Ma) Southern Volcanics, late Eocene (41–36 Ma) Northern Volcanics andMiocene–Pliocene (~5·0 Ma) Rangitihi Volcanics (Fig. 2).

The late Cretaceous Southern Volcanics are volumetrically the most significant and widely distributed group. The Southern Volcanics consist of lava flows 2–5 m thick that often show reddened brecciated bases and scoriaceous tops indicative of subaerial emplacement. Exposed lava sequences, up to 300 m thick, occur on the southern coast of Chatham Island and thin progressively to the north, consistent with a southern source located in the Pitt Strait (Morris, 1985*a*; Campbell *et al.*, 1993).

The late Eocene Northern Volcanics form small (<150 m in height) but prominent hills on the northern half of Chatham Island (Fig. 2). The hills represent variably eroded cones composed predominantly of interbedded basaltic lavas and pyroclastics. At Mairangi cone, reddened scoriaceous deposits containing bomb and block ejecta were produced by Strombolian activity. At Matakitaki cone, dark green palagonitized tuffs containing vesiculated lapilli-sized sideromelane fragments were produced by phreatomagmatic activity.

The Miocene–Pliocene Rangitihi Volcanics are concentrated in two areas on the northern coast of Chatham Island (Fig. 2). The deposits exposed at Cape Young and Maunganui consist of interbedded tuffs and tuff-breccias,

lavas and fossiliferous marine sediments. The Rangitihi Volcanics are characterized by megacrysts of amphibole (up to 4 cm in length) and also contain abundant crustal and mantle xenoliths. The presence of tuffaceous foraminiferan packstone surrounding and interclated with lobes of pillow basalts at the base of the volcanic sequence at Maunganui suggests that volcanic activity began with shallow submarine eruptions (Campbell *et al.*, 1993).

SAMPLE DESCRIPTION AND ANALYTICAL TECHNIQUES

This study is based on 36 mafic igneous rocks from the Campbell, Antipodes and Chatham island groups. The majority of the samples were collected from lava flows and small shallow intrusions. Most of the samples are dense, holocrystalline and porphyritic with phenocrysts of olivine and clinopyroxene (Table 1). Plagioclase feldspar is abundant (10–20%) as phenocrysts in Campbell Island lavas and is also the dominant interstitial phase in gabbro. Magnetite along with plagioclase occurs in the groundmass of most samples (Table 1) and kaersutite is found in Pliocene basalts from Chatham Island and in Pleistocene lavas from Antipodes Island (Gamble *et al.*, 1986). Dense holocrystalline samples are fresh and unaltered but some glassy and more vesicular samples show secondary alteration. Devitrification of hypohyaline groundmasses is observed in some lavas and blocks of the Northern Volcanics, including a palagonitized sideromelane tuff from Matakitaki cone on Chatham Island.

Thirty-two samples were analyzed for major and trace elements (V, Cr, Ni, Cu, Zn, Ga, Rb, Sr, Y, Zr, Nb, Ba and Pb) by X-ray fluorescence (XRF) on a Philips PW2400 XRF spectrometer at New Mexico Tech. Analytical precisions on major elements with concentrations >1 wt % are <0·1% (1σ) and for trace elements typically <4% (1σ). Lead concentrations for 12 samples were determined by inductively coupled plasma mass spectrometry (ICP-MS) with precisions of 1–2%, others by XRF with precisions of ~10% (Table 2). Other trace elements were measured at New Mexico Tech by instrumental neutron activation analysis (INAA) using 26% and 18% efficient high-purity Ge detectors (Hallett & Kyle, 1993). Based on repeat analyses of standards, we estimate analytical precision to be <1% for Sc, La, and Sm; <3% for Ce, Eu, Hf, Ta, Th and Lu; <5% for Tb and Yb; and <10% for Nd, Cs, and U.

Many of the Chatham Island samples have loss on ignition (LOI) values that exceed 1·0 wt % (Table 2). There is a broad correlation between higher LOI values and samples that contain glass and amygdules. However, only when considering the Northern Volcanics are correlations found between LOI and some major and trace elements. The geochemistry of the most highly altered samples (LOI >5 wt %), is not considered in subsequent petrogenetic discussions. For the remaining samples, major and trace elements were recalculated to 100% volatile-free (Table 2).

Sr, Nd and Pb isotopic analyses of 18 samples (Table 4) were performed at the Woods Hole Oceanographic Institution using conventional thermal ionization mass spectrometry (TIMS; Hauri & Hart, 1993). All sample chips were first leached in warm 6N HCl for 1 h before dissolution. Precisions of the Sr and Nd data are ± 0·003–0·005% (2σ). Reproducibility of Pb data is 0·05% per a.m.u. based on repeat runs of NBS981.

A total of 12 Chatham Island samples were dated by the $^{40}Ar/^{39}Ar$ method (Table 3). The whole-rock samples were crushed, sieved, leached with dilute HCl, washed in distilled water and hand-picked to remove phenocrysts and altered material to produce a groundmass concentrate. Amphibole separates were prepared by hand-picking crushed rock with the aid of a binocular microscope. The samples and Fish Canyon Tuff sanidine monitor (age 27·84 Ma) were irradiated for 14 h at the Nuclear Science Center reactor, College Station, Texas. Argon isotopic compositions of samples and monitors were determined at the New Mexico Geochronological Laboratory.

RESULTS

$^{40}Ar/^{39}Ar$ geochronology—Chatham Island

Twelve $^{40}Ar/^{39}Ar$ dates of basalts were obtained to better constrain the volcanic history of Chatham Island. Apparent ages were determined from age spectra and isotope correlation ($^{36}Ar/^{40}Ar$ vs $^{39}Ar/^{40}Ar$) diagrams (Table 3). The latter provide a quantitative measure of the initial argon composition and allow the identification of excess argon that has $^{40}Ar/^{36}Ar$ ratios greater than the present-day atmospheric value of 295·5. The $^{40}Ar/^{36}Ar$ intercept values in Table 3 indicate that excess argon is not significant in Chatham Island samples. The anomalous $^{40}Ar/^{36}Ar$ ratios for amphibole are a consequence of high uncertainties in the fit of the regression line. In all cases, the plateau age spectrum is interpreted to represent the eruption age of the basalts (Table 3 'preferred age' and Fig. 3). Degassing of the three amphibole samples occurred over a very narrow range of temperatures, which resulted in a small number of steps comprising >90% of the total $^{39}Ar_K$ released. Sample CHT-5 degassed primarily in one temperature step (1200°C, $^{39}Ar_K$ = 91·7%) and, therefore, does not meet plateau criteria (Fig. 3b). Its age, however, is indistinguishable from the plateau age for sample CHT-8, which was collected from a stratigraphically and lithologically equivalent unit. Alteration is the likely reason for the

Table 2: Major and trace element compositions of Chatham Island (CHT), Campbell Island (OU) and Antipodes Island (ANT) basalts

Sample:	CHT-1	CHT-3	CHT-5	CHT-8	CHT-9	CHT-10	CHT-11	CHT-12	CHT-14	CHT-16	CHT-17	CHT-18	CHT-20	CHT-21	CHT-22	CHT-23	CHT-24
Rock type:	akb	akb	basanite	basanite	trans bas	basanite	basanite	trans bas	BTA	tephrite	tephrite	akb	basanite	trans-bas	trans-bas	trans-bas	trans-bas
Unit:	ps	ps	mr	mr	kn	kn	kn	ps	kn	mr	mr	kn	mr	ps	ps	ps	ps
Age (Ma):	84·24	84·20	4·96	4·98	—	—	31·84	85·45	—	—	4·35	—	4·96	83·96	85·37	—	—
SiO_2	44·85	45·03	42·63	43·06	45·65	43·16	43·10	45·91	55·29	42·78	42·59	43·86	43·56	46·15	46·56	45·82	46·08
TiO_2	3·36	3·33	3·47	3·49	3·29	4·23	4·24	3·55	2·06	3·54	3·53	3·71	3·27	3·79	3·71	3·81	3·65
Al_2O_3	12·26	12·26	14·29	14·33	15·38	10·42	10·38	13·23	15·82	15·01	15·21	14·61	12·60	13·65	14·31	12·79	12·08
FeO†	13·04	12·98	12·85	12·57	12·78	13·29	13·28	13·75	8·23	14·23	14·18	13·25	12·58	12·58	12·23	12·77	12·85
MnO	0·20	0·19	0·18	0·18	0·20	0·19	0·19	0·19	0·15	0·23	0·24	0·18	0·17	0·19	0·19	0·19	0·20
MgO	11·23	11·26	9·48	9·04	7·68	12·34	12·12	9·44	4·71	6·24	5·82	8·38	12·49	8·47	8·01	9·57	10·27
CaO	9·15	9·06	11·88	12·09	10·75	11·33	11·43	8·77	6·68	11·29	11·17	11·84	11·98	10·44	9·77	10·97	11·16
Na_2O	3·26	3·27	3·04	3·08	2·37	2·40	2·60	2·58	3·96	3·34	3·87	2·38	2·10	2·63	2·89	2·38	1·97
K_2O	1·55	1·53	1·50	1·47	1·09	1·67	1·69	1·73	2·36	2·10	2·13	1·17	0·81	1·33	1·52	0·99	1·10
P_2O_5	1·10	1·08	0·68	0·68	0·81	0·97	0·98	0·85	0·74	1·24	1·25	0·62	0·43	0·76	0·82	0·69	0·64
LOI	0·73	0·72	1·99	1·89	3·83	2·36	2·32	1·72	2·42	3·35	2·65	2·93	2·35	1·27	1·45	1·96	2·62
Orig. sum	98·93	99·98	98·69	98·97	99·50	98·87	100·05	98·80	99·24	99·41	99·01	99·52	98·81	98·55	98·26	99·84	99·86
Mg-no.	63	63	59	59	54	65	64	58	53	46	45	56	66	57	56	60	61
Olivine %	21·9	21·6	26·2	26·4	31·5	19·9	20·3	29·7	22·5	43·1	44·6	31·0	16·8	28·1	28·1	25·5	23·8
ne	4·6	4·2	10·7	10·2	—	5·5	6·9	—	—	10·4	13·5	2·9	3·8	—	—	—	—
hy	—	—	—	—	6·7	—	—	4·3	10·9	—	—	—	—	3·6	2·9	5·5	9·6
ol	18·1	18·3	11·8	10·4	7·9	14·4	13·6	13·7	—	9·0	7·9	10·9	17·2	8·4	8·9	8·3	6·8
Q	—	—	—	—	—	—	—	—	4·8	—	—	—	—	—	—	—	—
Sc	18·8	18·4	25·4	26·3	19·2	21·0	20·9	22·1	12·6	14·9	14·8	25·0	29·1	24·3	21·9	26·5	27·7
V	230	225	320	331	283	249	242	226	130	318	311	335	320	301	274	298	295
Cr	394	378	212	205	143	320	315	233	116	13	14	176	490	279	242	406	538
Ni	334	345	130	140	103	370	362	209	90	28	26	99	257	153	126	195	245
Cu	45	48	87	89	60	71	70	42	27	62	62	74	80	62	48	67	70
Zn	135	134	120	118	141	150	145	144	132	178	177	126	104	124	124	117	114
Ga	23	24	21	22	23	23	22	25	24	26	28	24	19	25	25	23	21
Rb	31	31	35	35	25	41	38	36	41	56	59	32	14	24	30	17	17
Sr	1083	1046	998	975	1121	892	884	977	946	1086	1110	998	672	835	899	760	660
Y	38	38	31	31	35	34	34	39	22	40	41	30	24	32	34	30	29
Zr	421	412	254	250	314	381	377	416	318	451	460	273	198	370	399	329	306
Nb	82	79	83	80	93	102	100	69	45	136	138	77	54	60	64	52	49
Cs	0·40	0·40	0·59	0·45	0·30	0·57	0·63	0·47	0·72	0·58	0·58	0·38	0·20	0·19	0·25	0·84	0·23
Ba	455	447	539	562	566	620	629	452	570	635	694	506	275	383	406	364	349
La	69·8	67·5	69·6	66·5	66·8	61·6	61·7	57·1	40·7	95·4	94·7	50·3	35·1	47·5	51·1	42·2	39·4
Ce	150·3	141·7	133·0	128·5	128·5	124·8	125·3	125·1	82·7	183·6	185·2	102·4	74·2	102·3	108·9	92·1	86·9
Nd	66·1	65·1	57·9	58·2	54·2	57·3	53·8	55·7	37·8	71·2	76·7	42·0	30·7	46·6	52·4	43·7	30·5
Sm	14·42	13·65	11·11	10·52	11·35	12·98	12·89	12·69	8·15	14·22	14·17	9·72	8·00	11·36	11·32	9·92	9·79
Eu	4·33	4·08	3·27	3·24	3·42	3·92	3·97	3·80	2·552	4·19	4·16	2·99	2·37	3·26	3·51	3·10	2·85
Tb	1·68	1·53	1·21	1·22	1·33	1·63	1·46	1·51	0·954	1·59	1·58	1·19	0·95	1·43	1·33	1·26	1·12
Yb	2·43	2·42	2·06	2·10	2·40	1·79	1·90	2·35	1·68	2·63	2·79	1·90	1·41	2·00	2·33	1·90	1·76
Lu	0·31	0·32	0·25	0·28	0·33	0·24	0·22	0·31	0·22	0·37	0·38	0·27	0·18	0·30	0·34	0·25	0·22
Hf	9·41	9·37	5·73	6·03	7·41	8·67	8·63	9·61	7·37	9·20	9·37	6·60	5·26	8·69	9·07	7·81	7·57
Ta	5·03	4·92	4·59	4·52	5·68	5·79	5·86	4·43	2·98	8·44	7·90	4·69	3·32	3·93	4·26	3·52	3·24
Pb	4·09	4·58	4·98	5·20	4·4	3·8	3·46	4·53	4·0	7·2	7·56	3·5	2·56	3·07	3·17	2·8	2·8
Th	6·88	6·84	8·28	8·21	7·37	6·41	6·42	6·48	4·67	11·44	11·67	5·65	4·15	4·57	5·44	4·50	3·89
U	1·77	2·08	2·40	1·85	1·22	1·15	2·10	1·82	1·36	2·79	2·54	1·31	0·91	1·51	1·52	1·69	1·04

Table 2: continued

Sample:	CHT-25	CHT-26	CHT-27	OU36163	OU36173	OU36181	OU39737	OU39796	ANT3	ANT7	ANT13	ANT16
Rock type:	trans bas	trans bas	trans bas	subalk	trans bas	subalk	Q-gabbro	trans bas	basanite	tephrite	basanite	basanite
Unit:	ps	ps	ps	—	—	—	—	—	—	—	—	—
Age (Ma):	84·40	—	82·33	7	7	7	16	7	0·5	0·5	0·5	0·5
SiO_2	45·90	47·00	46·11	48·01	49·83	49·62	51·35	46·73	43·17	43·99	41·96	43·15
TiO_2	3·40	3·78	3·44	3·44	2·55	2·84	2·11	2·91	4·11	3·50	4·42	4·64
Al_2O_3	12·21	14·99	12·28	16·77	15·98	16·17	15·10	12·65	11·48	13·86	12·70	13·13
FeO^t	12·82	12·52	12·65	12·00	12·12	12·15	11·04	12·52	15·67	13·60	15·92	15·46
MnO	0·19	0·19	0·19	0·16	0·18	0·19	0·16	0·18	0·20	0·21	0·22	0·20
MgO	10·94	6·35	10·61	4·97	5·42	4·82	7·02	11·43	9·88	6·48	8·78	8·19
CaO	10·39	9·89	10·64	9·23	7·86	8·88	9·13	9·92	11·88	10·25	11·97	10·90
Na_2O	2·31	2·78	2·47	3·55	3·95	3·64	3·04	2·32	2·33	5·13	2·53	2·83
K_2O	1·20	1·68	1·00	0·88	1·40	1·00	0·72	0·85	0·76	1·72	0·74	0·88
P_2O_5	0·64	0·81	0·62	0·96	0·71	0·69	0·31	0·47	0·52	1·27	0·77	0·60
LOI	1·46	2·13	1·36	0·52	0·32	0·24	0·0	−0·17	−0·18	0·16	−0·33	−0·42
Orig. sum	99·80	99·64	99·54	99·72	99·38	100·16	99·63	100·16	100·24	100·3	98·42	99·69
Mg-no.	63	50	62	45	47	44	56	64	56	49	52	51
Olivine %	21·8	35·2	22·0	39·4	37·4	39·0	26·0	19·2	35·9	39·5	40·6	40·8
ne	—	—	—	—	—	—	—	—	3·0	16·2	4·4	3·1
hy	3·2	7·3	3·0	11·9	7·6	13·3	18·5	8·6	—	—	—	—
ol	13·8	3·3	12·7	—	6·6	—	—	12·9	13·4	7·5	11·9	10·6
Q	—	—	—	0·2	—	0·3	1·9	—	—	—	—	—
Sc	24·5	19·2	24·2	17·9	17·9	19·2	20·1	23·6	32·4	13·1	27·7	23·7
V	275	258	259	210	139	173	152	226	351	173	330	287
Cr	459	118	414	46	96	92	141	417	365	95	223	161
Ni	245	83	308	37	87	73	157	277	148	93	138	75
Cu	66	55	68	27	52	54	85	64	44	46	99	30
Zn	121	124	117	100	129	128	104	113	135	184	143	127
Ga	22	26	21	24	25	23	24	20	22	25	24	23
Rb	24	32	13	20	28	20	20	20	17	47	15	18
Sr	787	1301	730	713	532	519	348	554	530	1238	783	712
Y	28	35	31	30	34	31	25	26	30	35	34	31
Zr	297	369	291	163	299	220	141	219	232	419	273	236
Nb	52	64	51	36	53	43	22	44	44	99	49	42
Cs	0·20	0·23	0·00	0·15	0·22	0·19	0·42	0·14	0·42	0·47	0·14	0·13
Ba	362	443	332	230	353	268	168	253	250	425	296	219
La	42·0	50·5	38·5	31·1	42·5	33·5	18·6	32·0	31·1	86·6	42·3	30·8
Ce	89·6	110·0	83·3	66·8	85·9	67·8	40·6	65·6	68·3	172·4	91·9	69·4
Nd	41·1	49·2	31·8	32·0	36·6	28·6	20·7	30·2	27·8	72·0	42·0	37·2
Sm	8·95	10·92	8·73	7·81	9·02	8·03	5·12	6·96	8·44	15·60	10·03	8·88
Eu	2·88	3·44	2·81	2·65	3·04	2·71	1·75	2·20	2·62	4·64	3·17	2·86
Tb	1·11	1·39	1·19	1·03	1·25	1·23	0·82	0·93	1·06	1·62	1·28	1·16
Yb	1·99	2·29	1·78	1·80	2·73	2·34	1·74	1·77	1·81	2·25	2·15	1·84
Lu	0·25	0·28	0·23	0·24	0·33	0·33	0·22	0·20	0·26	0·25	0·25	0·22
Hf	7·20	8·50	6·73	4·24	6·75	5·51	3·79	5·24	5·93	8·96	6·15	6·13
Ta	3·54	4·33	3·19	2·59	3·51	2·84	1·74	2·91	3·26	6·41	3·33	3·29
Pb	2·90	4·1	2·82	1·4	3·0	2·0	1·5	1·5	1·3	6·0	1·1	0·5
Th	4·39	5·31	3·88	3·40	4·42	3·60	2·59	4·00	2·90	9·25	3·46	2·50
U	1·44	2·21	1·25	1·24	1·55	0·94	0·89	1·06	0·90	2·90	0·95	0·64

Chatham units: ps, Southern Volcanics; kn, Northern Volcanics; mr, Rangitihi Volcanics (Grindley *et al*., 1977). Chatham ages (Ma) determined by the $^{40}Ar/^{39}Ar$ method (Table 3). Ages for the Campbell and Antipodes Islands are from Cullen (1969), Adams *et al*. (1979) and Morris (1984). Major (wt %) and trace elements (ppm) are normalized to 100% anhydrous with total Fe as FeO^t ($FeO = 0{\cdot}9\ Fe_2O_3$). CIPW values for *ne*, *hy*, *ol* and *Q* are weight normative. LOI is the weight per cent loss of sample powder on ignition at 1000°C for 2 h. Mg-number is the atomic per cent $Mg^{2+}/(Mg^{2+} + Fe^{2+})$ and Olivine is the per cent of equilibrium olivine added incrementally to bring Mg-number to 73. Akb, alkali basalt; trans-bas, transitional basalt; BTA, basaltic trachyandesite; subalk, subalkali basalt (see text for classification details). Pb values with two significant figures were measured by isotope dilution (ICP-MS) with precision of ±1–2%. Other Pb values were measured by XRF (one significant figure) with precision of ±10%.

Table 3: Summary of $^{40}Ar/^{39}Ar$ data for Chatham Island basalts

Sample	Locality	Rock type	Sample	Total gas age (Ma)	±2σ	Plateau age (Ma)	±2σ	*n**	MSWD	^{39}Ar (%)	K/Ca	Isochron age (Ma)	±2σ	MSWD	$^{40}Ar/^{36}Ar$†	±2σ
CHT-1	Ohira Bay	akb	gm	84·1	3·9	*84·16*	*0·73*	8	1·3	98·7	0·6	84·30	0·88	1·2	295	2
CHT-3	Ohira Bay quarry	akb	gm	83·5	3·0	*84·09*	*0·96*	8	2·3	99·0	0·6	84·2	1·2	2·1	295	3
CHT-5	Cape Young	bas	amp	4·94	0·23	*4·96*	*0·25*	2	4·4	96·0	0·2	4·61	0·73	11·0	460	199
CHT-8	Cape Young	bas	amp	5·27	0·16	*4·97*	*0·10*	2	0·7	98·5	0·2	5·02	0·63	20·0	270	268
CHT-11	Mt. Chudleigh	bas	gm	43·4	14·0	36·0	4·2	9	3·4	100·0	2·0	*32·1*	*4·8*	2·0	299	3
CHT-12	Waitaha Creek	akb	gm	84·5	3·3	*85·45*	*0·59*	7	1·5	93·0	0·5	85·50	0·73	1·5	295	2
CHT-17	Maunganui	bas	gm	5·0	1·9	*4·34*	*0·45*	5	8·4	76·0	1·3	4·5	1·5	20·0	291	27
CHT-20	Tawreikoko	akb	gm	19·0	16·3	7·3	3·3	8	2·1	96·7	0·3	*5·3*	*3·0*	1·8	299	3
CHT-20	Tawreikoko	akb	amp	5·07	0·34	*4·95*	*0·27*	3	3·0	98·9	0·2	4·95	0·34	4·6	296	47
CHT-21	Tuku River	akb	gm	83·8	2·3	*84·01*	*0·86*	8	3·9	99·4	0·4	84·00	0·90	4·7	295	5
CHT-22	Tuku River	akb	gm	85·8	1·9	*85·37*	*0·60*	6	2·1	90·2	0·5	85·30	0·61	2·3	297	4
CHT-25	Tuku River	akb	gm	85·1	3·0	*84·5*	*1·4*	8	8·9	99·4	0·4	84·4	1·4	8·1	297	6
CHT-27	Cape Fournier	akb	gm	81·0	5·8	*82·26*	*0·79*	7	1·5	93·0	0·3	82·41	0·91	1·3	295	2

*Number of apparent ages included in the mean plateau age calculation.
†Value of *y*-intercept on inverse isochron plots.
Preferred ages are shown in italics. akb, alkali basalt; bas, basanite; gm, groundmass; amp, amphibole (kaersutite). Measurements were made using a Mass Analyzer Products 215-50 mass spectrometer operated in electron multiplier mode with an overall sensitivity of $\sim 3{\cdot}0 \times 10^{-17}$ moles/pA. Samples were step-heated in a double-vacuum molybdenum resistance furnace. Typical blanks including mass spectrometer backgrounds were 171, 4, 0·1, 0·8 and $0{\cdot}8 \times 10^{-18}$ moles at masses 40, 39, 38, 37 and 36, respectively. *J*-factors were determined to a precision of 0·10% by analyzing four single-crystal aliquots from each of 4–6 radial positions around each Al irradiation tray. Corrections for interfering nuclear reactions were determined using K-glass and CaF_2. These values are $(^{40}Ar/^{39}Ar)_K = 0{\cdot}0002 \pm 0{\cdot}0002$, $(^{36}Ar/^{37}Ar)_{Ca} = 0{\cdot}00026 \pm 0{\cdot}00002$ and $(^{39}Ar/^{37}Ar)_{Ca} = 0{\cdot}00070 \pm 0{\cdot}00005$. All errors are reported at the 2σ confidence level. Decay constant and isotopic abundances follow Steiger & Jäger (1977).

discordant age spectrum of groundmass samples CHT-11 and CHT-20. The low radiogenic ^{40}Ar yields caused by alteration translate into high uncertainties on the age of individual temperature steps. Radiogenic yields are significantly higher for amphibole separated from CHT-20, providing an apparent age with a higher precision (Table 3).

The $^{40}Ar/^{39}Ar$ ages provide several important modifications to the volcanic history of Chatham Island based on the K–Ar dates of Grindley *et al.* (1977). Our results indicate that the late Cretaceous volcanism, which produced the Southern Volcanics, is significantly older than previously thought. The $^{40}Ar/^{39}Ar$ age determinations from this study range from 82·26 ± 0·79 Ma to 85·45 ± 0·59 Ma whereas prior K–Ar dates range from 70·4 ± 1·2 Ma to 81·4 ± 2·0 Ma [revised using the decay constants and isotopic abundances recommended by Steiger & Jäger (1977)]. Our samples were collected from units that encompass most of the volcanic stratgraphy of Chatham Island and from some of the same sites sampled for K–Ar dating. Two basalts collected ~1 km apart on the same lava flow at Ohira Bay yield indistinguishable $^{40}Ar/^{39}Ar$ ages of 84·16 ± 0·73 Ma and 84·2 ± 1·2 Ma (samples CHT-1 and CHT-3, respectively; Table 3). These ages are significantly older than the revised K–Ar age of 79 ± 2·0 Ma [sample R3198 of Grindley *et al.* (1977)] from the same flow. Other locations where our results yield significantly older ages relative to previous K–Ar ages include samples collected from Waitaha Creek (CHT-12) and Cape Fournier (CHT-27). We, therefore, conclude that the age of the Southern Volcanics from the Chatham Islands are more tightly clustered around 84–85 Ma rather than the younger and longer (~10 Myr) time-span proposed by Grindley *et al.* (1977). A relatively short period of eruption for the bulk of the Southern Volcanics is supported by the age of samples collected from the base and top of thick (80–100 m) lava sequences that are indistinguishable within the resolution of argon dating.

The Cenozoic volcanism on the Chatham Islands consists of at least 10 separate volcanic lithostratigraphic units, only half of which have been dated by radiometric methods (Campbell *et al.*, 1993). Previous K–Ar ages for the Northern Volcanics are late Eocene (41–36 Ma). In this study, one sample of the Northern Volcanics collected from Mt. Chudleigh (Fig. 2) has a slightly younger age of 32·1 ± 4·8 Ma (CHT-11). Four samples of the Pliocene–Miocene Rangitihi Volcanics were dated by

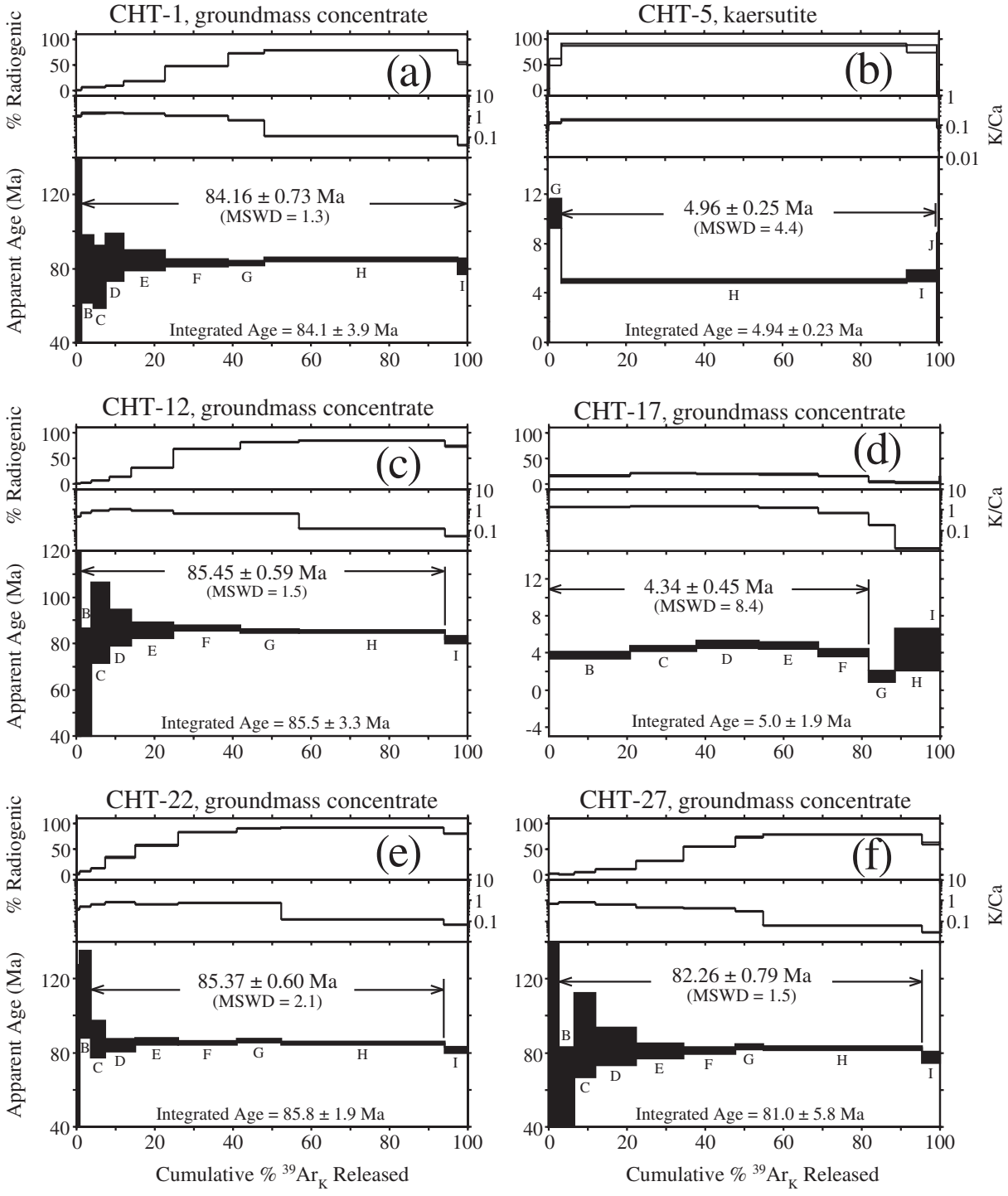

Fig. 3. Representative $^{40}Ar/^{39}Ar$ ages for Chatham Island basalts. (a–f) Age release, K/Ca and radiogenic argon release ($^{40}Ar^*$) spectra of groundmass and amphibole fractions. Thicknesses of boxes represent 2σ error.

the $^{40}Ar/^{39}Ar$ method and generally agree with previous K–Ar ages. Two amphibole separates from basaltic lavas at Cape Young yield indistinguishable ages of 4·96 ± 0·25 Ma and 4·97 ± 0·10 Ma (CHT-5 and CHT-8, respectively; Table 3). Approximately 12 km to the west at Maunganui (Fig. 2), a lava flow on the coast is dated at 4·34 ± 0·45 Ma (CHT-17, Fig. 3d). Our $^{40}Ar/^{39}Ar$ age determinations indicate that Rangitihi Volcanics also

exist at the Tawreikoko volcanic cone (Fig. 2). Tawreikoko cone is composed of breccias and lavas mapped as Northern Volcanics but is cut by a kaersutite-bearing basaltic dike of Rangitihi age (4·95 ± 0·27 Ma, CHT-20 amp, Table 3).

Major and trace elements

Mafic igneous rocks from the Chatham, Antipodes and Campbell islands range in composition from ultrabasic to basic (42–51 wt % SiO_2), have Mg-numbers between 44 and 65, and are classified as basanite (*ne*-normative, >10% *ol*-normative), tephrite (*ne*-normative, <10% *ol*-normative), alkali- and transitional basalts (<10% *hy*-normative), subalkali basalt, and *Q*-gabbro (>10% *hy*-normative, *Q*-normative) according to the recommendations of Le Maitre (2002). One sample from Chatham Island (CHT-14) is intermediate in composition and classified as a basaltic trachyandesite (Table 2).

The broad correlation of MgO with major and trace elements displayed in Fig. 4 suggests that most of the samples have been modified by crystal fractionation. The fractionation of olivine is indicated by increasing Al_2O_3 and decreasing Ni (not shown in Fig. 4) ($K_D^{ol/melt}$ Ni 10–23, Hart & Davis, 1978), whereas fractionation of clinopyroxene is indicated by decreasing MgO with CaO/Na_2O and Cr ($K_D^{Cpx/melt}$ Cr 3·8, Hart & Dunn, 1993). A negative correlation between Zr/Hf ratios and Sc content, particularly well defined in the Southern Volcanics, is also indicative of clinopyroxene control during crystallization (David *et al.*, 2000).

With decreasing MgO the Rangitihi Volcanics show a systematic increase in the concentration of most incompatible elements (e.g. Ba, Nb, La, Th) and depletion in elements compatible with olivine and clinopyroxene (Fig. 4). The trend of increasing FeO^t with decreasing MgO (not shown) argues against significant fractionation of Fe–Ti oxides. The slight decrease in SiO_2 with MgO (Fig. 4) and corresponding increase in Si-undersaturation (from ~4% to >10% normative nepheline, Table 2) is in response to the removal of kaersutite; a Ti-rich, silica-poor amphibole that is found in high modal proportions in the Rangitihi Volcanics (Table 1). The fractionation of kaersutite has also buffered TiO_2 concentrations. TiO_2 will increase with crystallization of olivine and clinopyroxene with little or no fractionation of Fe–Ti oxides; however, the high TiO_2 content of kaersutite (~5 wt %) relative to the magma (~<3 wt %) counteracts this affect. Removing kaersutite from the magma also depletes Ti relative to middle rare earth elements (MREE), Eu and Tb (Ti/Ti*, Fig. 4) and other large ion lithophile elements (LILE). The coherent fractionation trends of Rangitihi Volcanics can be modeled by the fractionation of 25% clinopyroxene, 19% kaersutite, 15% olivine, 10% plagioclase and 4% titanomagnetite from the least fractionated basanite (CHT-20, MgO >12 wt %) to produce a 27% residual that closely approximates the major element ($\sum r^2 = 0{\cdot}04$) and trace element concentrations (errors for U and Th <20%, Zr, Hf, Ba <15% and Sr, La, Ce, Ta, Nb <10%) of tephrite (CHT-17, MgO <6 wt %). This least-squares mass balance and Rayleigh fractionation model uses mineral analyses from the Rangitihi Volcanics and the mafic mineral–melt partition coefficients of Caroff *et al.* (1993). Mass balance models for other suites suggest that clinopyroxene and olivine (± plagioclase) controlled the evolution from alkali basalt to hawaiite for the late Cretaceous and Eocene sequences on Chatham Island (Morris, 1985*a*, 1985*b*). Morris (1984) also modeled the differentiation of transitional basalt to hawaiite on Campbell Island by the removal of plagioclase and lesser amounts of clinopyroxene, consistent with the observed petrography.

To help evaluate the source of the basalts and constrain partial melting processes we have selected the most primitive samples from each island. Seven of the basalts are relatively unfractionated (Mg-number 62–66, Cr > 300 ppm and Ni > 250 ppm); these include one sample from Campbell Island (OU39796) and one from each of the three main age-delimited volcanic groups on Chatham Island. The least fractionated Antipodes Island sample (ANT-3) is comparable in concentration with respect to Al_2O_3, CaO, Cr and V but has a lower Mg-number (56) and lower Ni (148 ppm) content, indicating that greater amounts of olivine have been fractionated. To compensate for olivine fractionation the samples were normalized to Mg-number 73. This was accomplished by adding olivine, incrementally, to each composition while maintaining a constant Fe^{2+}/Mg K_D value equal to 0·30 until the Mg-number reached 73 and olivine reached Fo_{90}. Trace element concentrations were reduced by the percentage of olivine added back to each composition (Table 2).

The olivine-normalized basanite, alkali- and transitional-basalts from the Antipodes, Campbell and Chatham Islands are compared on multi-element and REE plots in Figs 5 and 6, respectively. The samples display similar enriched trace element patterns with peaks at Na–Ta and prominent negative K- and Pb-anomalies (Fig. 5). The basalts also show parallel and moderately steep patterns on REE plots with La_N/Yb_N values between 12 and 28 and La_N/Sm_N values between 2·4 and 3·2 (Fig. 6), which implies that all of the basalts are the products of small melt fractions of a garnet-bearing source. A notable difference, however, is evident in their relative Ti concentrations (Fig. 5). The Ti/Ti* values for the basalts are variable (0·8–1·7) and span this range of values in samples from all localities (Fig. 4). There is also a difference in Zr/Nb and Hf/Nb values between the Late Cretaceous (Zr/Nb = 5·2–5·8, Hf/Nb = 0·12–0·13) and

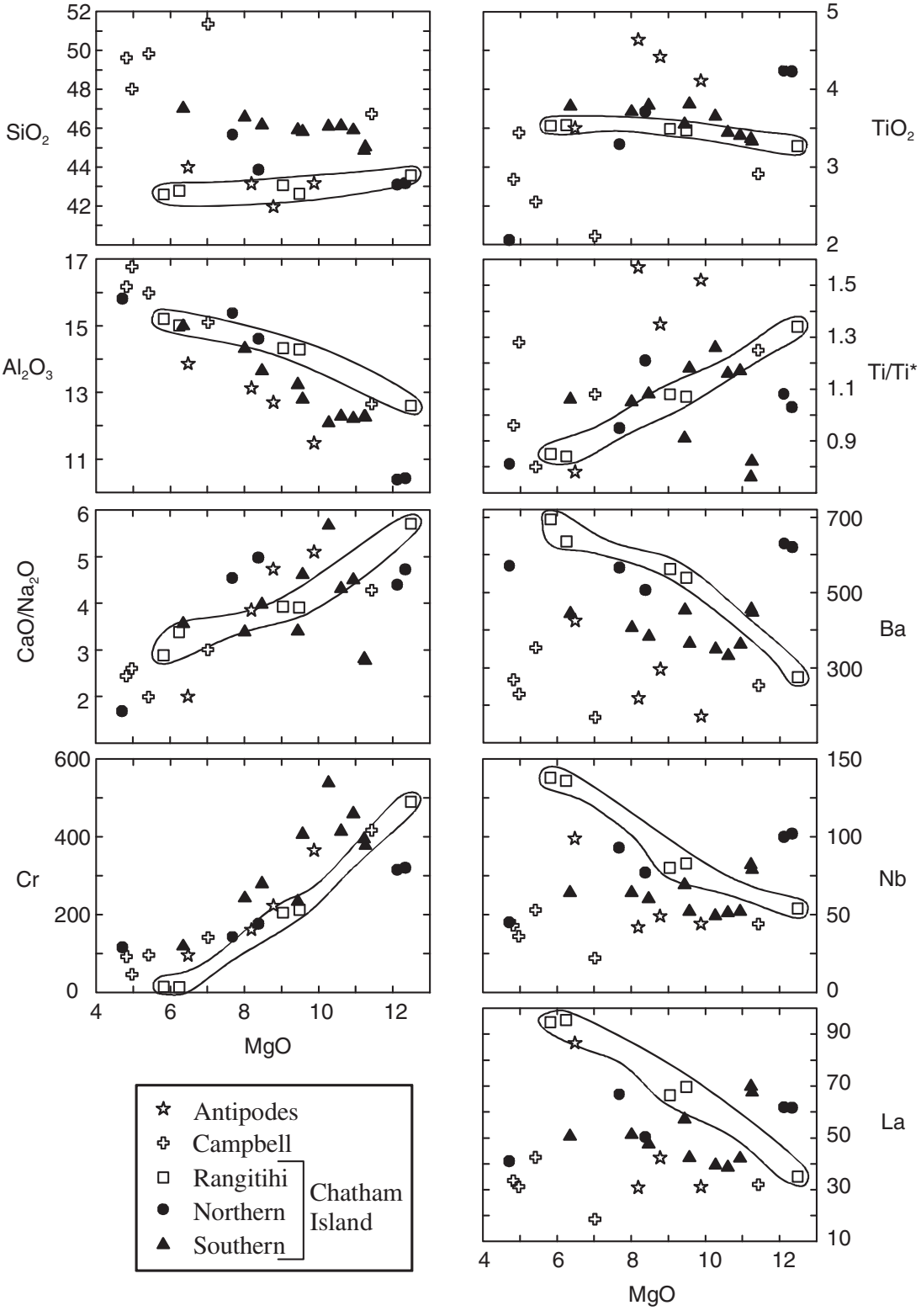

Fig. 4. Variations in major and trace elements with MgO (wt %). Ti/Ti* is the ratio between Ti concentration and the values interpolated between adjacent elements, Eu and Tb, on primitive mantle normalized multi-element diagrams as shown in Fig. 5. Trends in Rangitihi basalts are considered evidence for progressive magmatic differentiation by mineral fractionation (see text).

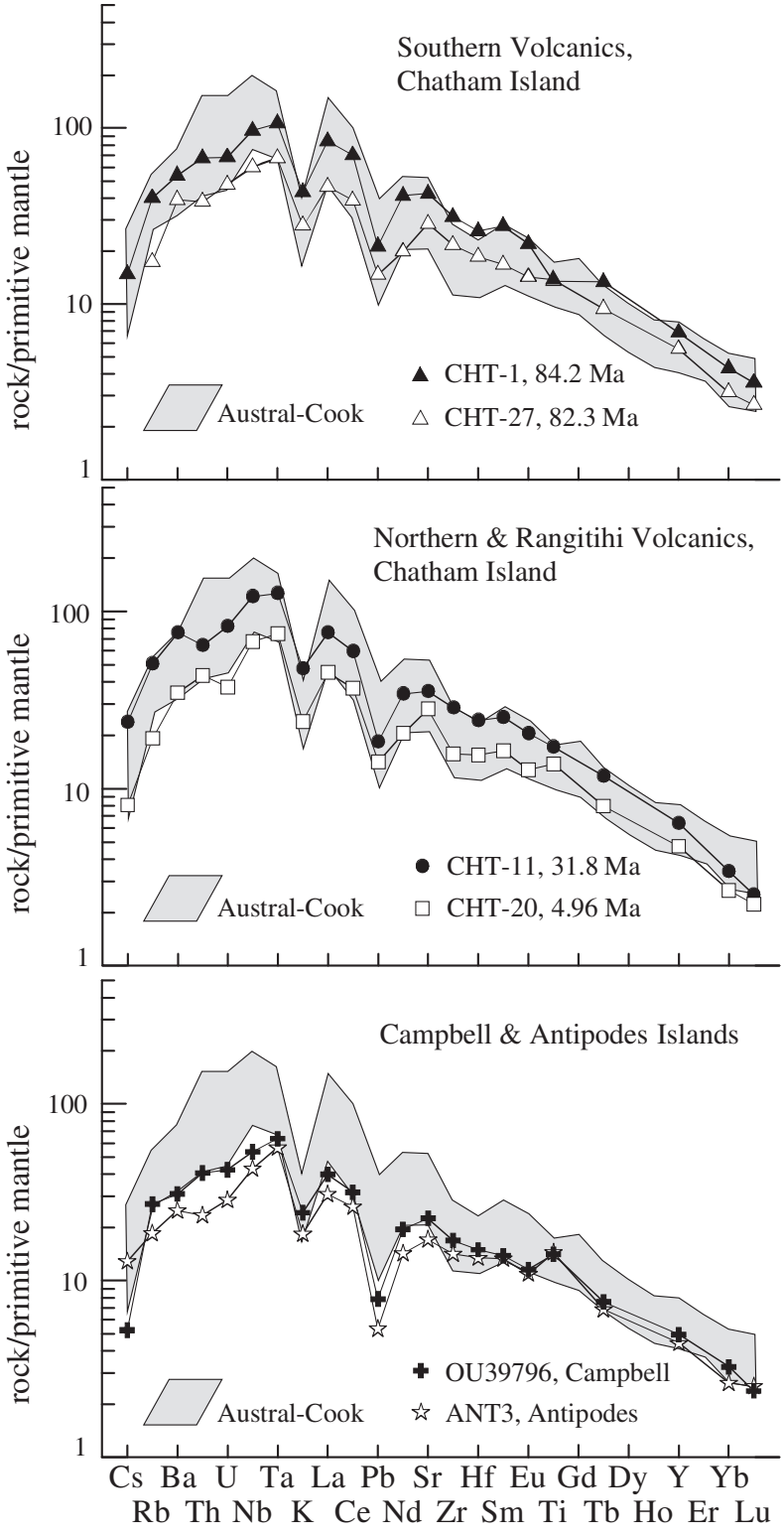

Fig. 5. Primitive mantle normalized trace element patterns of primitive basalts from the Antipodes, Campbell and Chatham Islands. The major and trace element concentrations of samples have been corrected for olivine fractionation and are normalized to the primitive upper mantle values of McDonough & Sun (1995). The shaded field encompasses young basalts with MgO >6·0 wt % from the Austral–Cook Islands and includes the islands of Mangaia and Tubuai (compiled from the GEOROC database; available at http://georoc.mpch-mainz.gwdg.de). The Austral–Cook samples were not corrected for olivine fractionation.

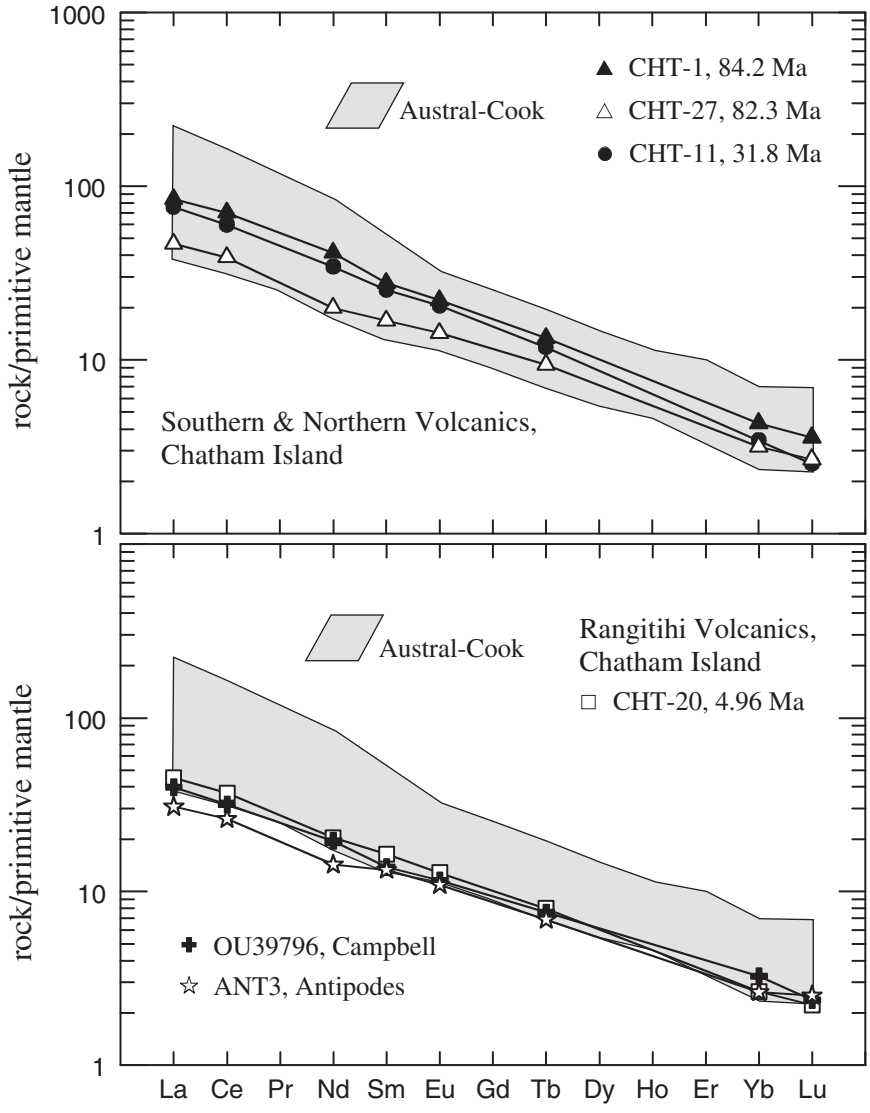

Fig. 6. Primitive mantle normalized rare earth element abundances for the same samples as shown in Fig. 5. Normalization values of McDonough & Sun (1995).

Cenozoic (Zr/Nb = 3·7–3·8, Hf/Nb = 0·09–0·10) basalts from Chatham Island. Setting aside these subtle variations it is apparent that the overall trace element characteristics (Fig. 5) and low LILE/Nb values (e.g. Fig. 7) of the New Zealand samples are comparable with those of other continental alkaline basalts from the SW Pacific (Johnson, 1989; Finn *et al.*, 2005) and OIB, in particular, those that have the HIMU type isotopic signature (St. Helena and the Austral–Cook island chain).

Sr, Nd and Pb isotopes

Results of isotope analysis for Chatham, Antipodes and Campbell island samples are presented in Table 4 and are plotted with reference to basalts from the south–central Pacific and South Atlantic oceans in Fig. 8. Also included in Fig. 8 are data for samples from alkaline magmatic suites on the South Island of New Zealand; the early Miocene Westland dike swarm (Barreiro & Cooper, 1987), mafic clasts within the Port Chalmers Breccia (PCB) of the Dunedin Volcanic Group (Price *et al.*, 2003), the mid-Cretaceous Tapuaenuku igneous complex (Baker *et al.*, 1994; J. A. Baker, unpublished data, 1997) and Auckland Island (J. A. Gamble & R. J. Wysoczanski, unpublished data, 2006). All data plotted in Fig. 8 are measured values. Although it is customary to correct for the radiogenic in-growth of daughter nuclides to discuss source signatures we suggest that a better comparison between Mesozoic and Cenozoic samples can be

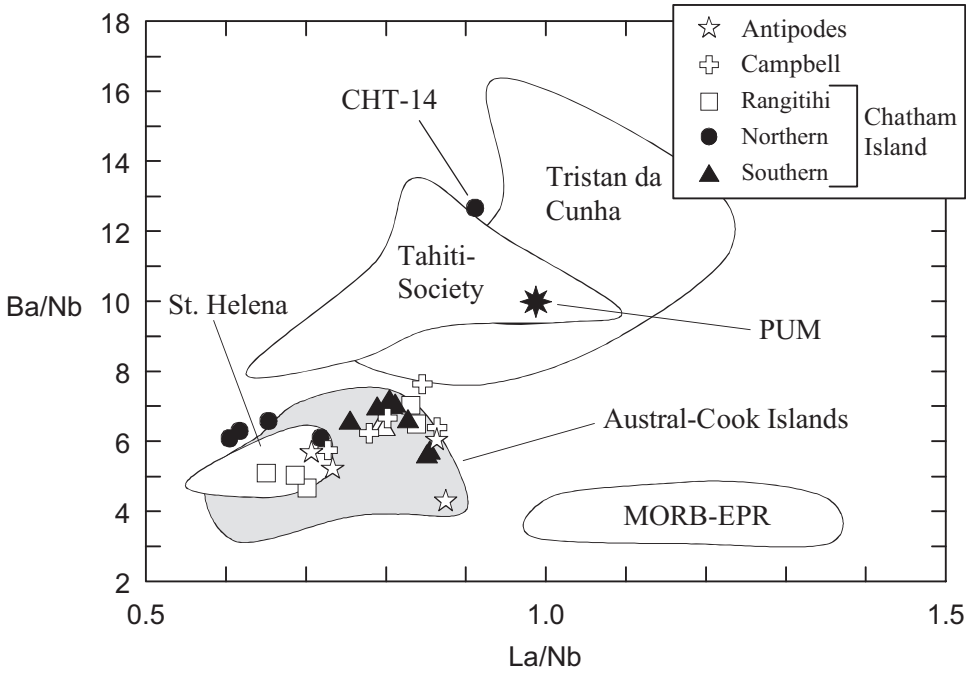

Fig. 7. Ba/Nb vs La/Nb ratios. Field for Austral–Cook Island basalts delimits the same data and sources as in Figs 5 and 6. Chatham Island sample CHT-14 is evolved and classified as a basaltic trachyandesite. PUM, Primitive Upper Mantle (McDonough & Sun, 1995). Mid-ocean ridge basalts (MORB) from the East Pacific Rise (EPR) compiled from the PETDB database (http://www.petdb.org/index.jsp).

made if the values are left uncorrected. We consider the measured values to be close approximations of their present-day source values. To evaluate this assertion, initial isotopic ratios for the Cretaceous Chatham Island basalts were projected to the present day using parent/daughter ratios calculated by means of a two-stage mantle evolution model. In Table 4, the model source ratios differ from measured ratios by $\leq$0·00008 for $^{87}Sr/^{86}Sr$, $\leq$0·00004 for $^{143}Nd/^{144}Nd$ and $\leq$0·19 for $^{206}Pb/^{204}Pb$.

Together, the basalts from the Chatham and subantarctic islands show a restricted range in measured $^{143}Nd/^{144}Nd$ (0·5128–0·5129) and $^{207}Pb/^{204}Pb$ (15·6–15·7) values, a moderate range in measured $^{87}Sr/^{86}Sr$ (0·7029–0·7040) and $^{208}Pb/^{204}Pb$ (39·1–40·5) values, and a wide range in measured $^{206}Pb/^{204}Pb$ values (19·2–20·8). With the exception of one sample (CHT-11) all Chatham Island and Antipodes Island basalts have high $^{206}Pb/^{204}Pb$ (20·3–20·8) and low $^{87}Sr/^{86}Sr$ ($\sim$0·703) values and define moderately tight clusters on isotope correlation plots (Fig. 8). In Fig. 8, the Chatham and Antipodes basalts mostly lie between the FOZO and HIMU mantle domains redefined by Stracke *et al.* (2005) based on oceanic basalts from the Austral–Cook island chain and St. Helena. The samples from Tapuaenuku and the Westland dike swarm show wider variations in $^{206}Pb/^{204}Pb$ and $^{208}Pb/^{204}Pb$ values, and along with the Dunedin samples (PCB), are intermediate between rocks from Campbell Island and those from the Chatham and Antipodes Islands. The gabbros from Tapuaenuku have the lowest $^{143}Nd/^{144}Nd$ values whereas the *Q*-gabbro and transitional to subalkaline basalts from Campbell Island have, on average, the highest $^{87}Sr/^{86}Sr$ values.

DISCUSSION

Crustal contamination

Continental alkaline basalts with high Sr isotope ratios and OIB-like trace element signatures are often attributed to small-degree melts of a metasomatically enriched mantle lithosphere (e.g. Baker *et al.*, 1997; Zhang & O'Reilly, 1997; Späth *et al.*, 2001; Barry *et al.*, 2003). High Sr isotope ratios in basalts may, however, reflect contamination from radiogenic crust. Chemical contributions from continental crust have previously been proposed for some of the mafic rocks from the Tapuaenuku igneous complex (Baker *et al.*, 1994) and for the Westland dike swarm (Barreiro & Cooper, 1987). In each case, the samples that have slightly elevated Sr isotope ratios (>0·7035, Fig. 8c) also have low Sr concentrations and, therefore, are more susceptible to contamination from highly radiogenic crust.

The transitional to slightly silica-oversaturated basalts from Campbell Island have elevated $^{87}Sr/^{86}Sr$ values and low Sr contents ($\sim$350–700 ppm) relative to Chatham and Antipodes samples ($\sim$700–1300 ppm, Table 2).

Table 4: Sr, Nd and Pb Isotope data for Chatham, Antipodes and Campbell Islands, New Zealand

Sample	Age (Ma)	$^{87}Rb/^{86}Sr$	$^{87}Sr/^{86}Sr$ (initital)	Model source	$^{147}Sm/^{144}Nd$	$^{143}Nd/^{144}Nd$ (initital)	εNd(t)	Model source	$^{206}Pb/^{204}Pb$ (initial)	Model source	$^{207}Pb/^{204}Pb$ (initial)	$^{208}Pb/^{204}Pb$ (initial)	μ	ω	κ
Chatham Island															
CHT-1	84·24	0·0829	0·703000 ± 15 (0·702901)	0·702945	0·1323	0·512836 ± 09 (0·512763)	4·6	0·512875	20·654 (20·307)	20·521	15·728 (15·712)	40·168 (39·725)	26·4	106·1	4·0
CHT-3	84·2	0·0858	0·703001 ± 16 (0·702900)	0·702944	0·1272	0·512832 ± 10 (0·512762)	4·5	0·512874	20·780 (20·411)	20·628	15·734 (15·716)	40·144 (39·746)	28·1	95·2	3·4
CHT-5	4·96	0·1016	0·703278 ± 19 (0·703270)		0·1164	0·512835 ± 11 (0·512831)	3·9		20·439 (20·417)		15·656 (15·655)	40·141 (40·116)	29·0	103·2	3·6
CHT-8	4·98	0·1039	0·703351 ± 16 (0·703343)		0·1097	0·512855 ± 10 (0·512851)	4·3		20·335 (20·318)		15·647 (15·646)	40·001 (39·977)	21·5	98·5	4·6
CHT-11	31·84	0·1245	0·703001 ± 16 (0·702944)		0·1453	0·512883 ± 11 (0·512853)	5·0		19·790 (19·608)		15·649 (15·640)	39·727 (39·544)	36·8	116·4	3·2
CHT-12	85·45	0·1067	0·703183 ± 18 (0·703052)	0·703102	0·1381	0·512825 ± 10 (0·512748)	4·3	0·512861	20·303 (19·980)	20·188	15·742 (15·727)	39·821 (39·443)	24·2	89·2	3·7
CHT-17	4·35	0·1539	0·703278 ± 21 (0·703268)		0·1120	0·512854 ± 10 (0·512851)	4·3		20·642 (20·628)		15·679 (15·679)	40·470 (40·449)	20·1	95·4	4·7
CHT-20	4·96	0·0603	0·703238 ± 24 (0·703233)		0·1581	0·512859 ± 10 (0·512854)	4·3		20·321 (20·305)		15·620 (15·619)	40·071 (40·046)	21·4	100·6	4·7
CHT-21	83·96	0·0832	0·703012 ± 19 (0·702913)	0·702958	0·1479	0·512830 ± 11 (0·512749)	4·3	0·512860	20·595 (20·204)	20·415	15·736 (15·718)	40·110 (39·723)	29·8	93·0	3·1
CHT-22	85·37	0·0966	0·702962 ± 21 (0·702843)	0·702886	0·1312	0·512845 ± 10 (0·512772)	4·8	0·512886	20·637 (20·252)	20·468	15·698 (15·680)	39·929 (39·476)	28·9	106·9	3·7
CHT-25	84·4	0·0883	0·703036 ± 18 (0·702931)	0·702976	0·1320	0·512835 ± 10 (0·512762)	4·5	0·512874	20·481 (20·079)	20·288	15·692 (15·673)	39·953 (39·553)	30·5	95·7	3·1
CHT-27	82·33	0·0516	0·702983 ± 21 (0·702920)	0·702964	0·1664	0·512832 ± 11 (0·512742)	4·1	0·512851	20·364 (20·017)	20·219	15·733 (15·717)	39·907 (39·552)	27·1	86·9	3·2
Antipodes and Campbell Islands															
ANT3	0·5	0·0946	0·702930 ± 20 (0·702929)		0·1842	0·512921 ± 10 (0·512920)	5·5		20·608 (20·604)		15·693 (15·693)	39·906 (39·894)	45·4	151·2	3·3
ANT13	0·5	0·0558	0·702934 ± 17 (0·702934)		0·1449	0·512913 ± 11 (0·512913)	5·4		20·532 (20·528)		15·657 (15·657)	39·739 (39·723)	56·0	210·8	3·8
ANT16	0·5	0·0724	0·702903 ± 15 (0·702902)		0·1448	0·512911 ± 10 (0·512911)	5·3		20·492 (20·485)		15·651 (15·651)	39·728 (39·700)	89·7	362·1	4·0
OU36163	7	0·0820	0·704047 ± 16 (0·704039)		0·1481	0·512843 ± 10 (0·512836)	4·0		19·230 (19·167)		15·664 (15·664)	39·326 (39·147)	58·1	164·6	2·8
OU39737	16	0·1662	0·703748 ± 21 (0·703710)		0·1352	0·512818 ± 10 (0·512804)	3·6		19·164 (19·067)		15·629 (15·628)	39·149 (38·858)	38·8	117·2	3·0
OU39796	7	0·1050	0·703671 ± 16 (0·703661)		0·1398	0·512875 ± 10 (0·512869)	4·7		19·340 (19·290)		15·603 (15·603)	39·235 (39·041)	45·9	178·9	3·9

Element concentrations are given in Table 3 and were determined by XRF (Rb, Sr), INAA (Sm, Nd, U, Th) and isotope dilution (Pb). Sr and Nd isotope interlab standard values were 0·71024 for Sr (NBS 987) and 0·511847 for Nd (La Jolla). Errors are 2σ. Nd isotopes normalized to $^{146}Nd/^{144}Nd$ of 0·7219. Pb analyses were corrected using NBS981 ($^{206}Pb/^{204}Pb$ 16·9356, $^{207}Pb/^{204}Pb$ 15·4891, $^{208}Pb/^{204}Pb$ 36·7006, Todt *et al.*, 1996). $\mu = {}^{238}U/{}^{204}Pb$, $\omega = {}^{232}Th/{}^{204}Pb$, and $\kappa = {}^{232}Th/{}^{238}U$. Source ratios were calculated using a two-stage mantle evolution model. For example, the present-day $^{143}Nd/^{144}Nd$ value of the source for late Cretaceous basalts is calculated by first determining the $^{143}Nd/^{144}Nd$ of Bulk Earth at 2·5 Ga (using $\lambda_{Sm} = 6{\cdot}54 \times 10^{-12}$, $^{143}Nd/^{144}Nd_{chur} = 0{\cdot}506697$ at 4·6 Ga, and $^{147}Sm/^{144}Nd_{chur} = 0{\cdot}1967$) and then projecting a line from this value through the initial $^{143}Nd/^{144}Nd$ ratio calculated for each sample. The intercept ($^{143}Nd/^{144}Nd$ at $t = 0$ Ma) and slope ($^{147}Sm/^{144}Nd$) of this line are the model source values. Model source $^{87}Sr/^{86}Sr$ ratios were calculated using $\lambda_{Rb} = 1{\cdot}42 \times 10^{-11}$, $^{87}Sr/^{86}Sr_{babi} = 0{\cdot}698990$ at 4·6 Ga, and $^{87}Rb/^{86}Sr = 0{\cdot}0871$. Model source $^{206}Pb/^{204}Pb$ ratios used $\lambda_U = 1{\cdot}55125 \times 10^{-10}$, $^{206}Pb/^{204}Pb = 9{\cdot}307$ at 4·6 Ga, and $^{238}U/^{204}Pb = 8{\cdot}670$. Model parent/daughter ratios are 0·202–0·204 for $^{147}Sm/^{144}Nd$, 0·035–0·041 for $^{87}Rb/^{86}Sr$ and 15·6–16·5 for $^{238}U/^{204}Pb$.

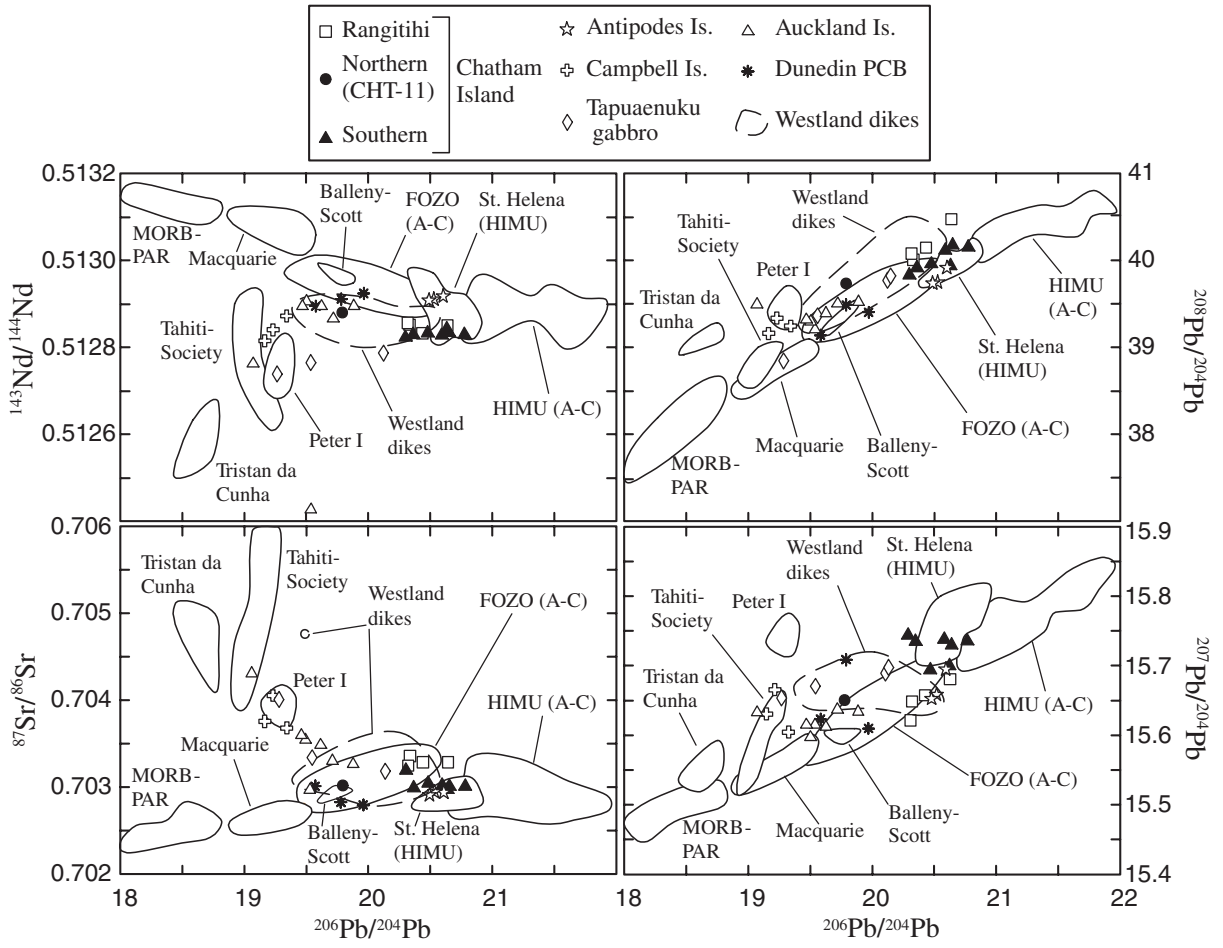

Fig. 8. $^{143}Nd/^{144}Nd$, $^{87}Sr/^{86}Sr$, $^{208}Pb/^{204}Pb$, $^{207}Pb/^{204}Pb$ vs $^{206}Pb/^{204}Pb$ isotope correlation plots of southern New Zealand basalts in comparison with oceanic basalts. Tapuaenuku gabbros are from Baker *et al.* (1994; J. Baker, unpublished data, 1997—Pb isotopes measured on leached feldspars and Sr and Nd are for whole-rocks). All of the data are plotted as measured values. The Westland dikes are lamprophyres, phonolites and carbonatites from Barreiro & Cooper (1987). Mafic clasts from the Port Chalmers Breccia (PCB), part of the Dunedin Volcanic Group, New Zealand, consist of *ne*-normative ultramafic cumulates, amphibole gabbro and basanite from Price *et al.* (2003). Basalts and gabbros from Auckland Island are from J. A. Gamble & R. J. Wysoczanski (unpublished data, 2006). Basalts from subantarctic islands Peter I (Hart *et al.*, 1995), Balleny and Scott (Hart *et al.*, 1992, 1995; Hart & Kyle, 1994) are also included. Data from St. Helena and the Austral–Cook Islands (A-C), including their classification as FOZO (FOcus ZOne; originally described by Hart *et al.*, 1992) and HIMU types, are from Stracke *et al.* (2005). MORB samples from the Pacific–Antarctic Ridge (PAR) 56–66°S are from Vlastélic *et al.* (1999). Macquarie Island mafic glasses (Mg-numbers 58–69) are from Kamenetsky *et al.* (2000).

They also have lower average Nb/U values (~34) relative to OIB (~47, Hofmann *et al.*, 1986) and Antipodes and Chatham island basalts (~46), which may indicate fractionation and addition of low Nb/U crust [10–20 for total continental crust (Sims & DePaolo, 1997) and ~5 for bulk metasediments from southern New Zealand (Mortimer & Roser, 1992)]. To evaluate the possibility that Campbell Island samples have been contaminated by crust we have modeled several evolutionary paths for combined assimilation and fractional crystallization (AFC) on isotope and trace element ratio plots (Fig. 9). A mildly fractionated basalt from Chatham Island (CHT-17) was selected for the starting composition and several possible assimilants, representing the pre-Cenozoic basement of New Zealand (Graham & Mortimer, 1992; Graham *et al.*, 1992) and modern near-trench bulk sediments collected from the Kermadec–Hikurangi margin to the north of New Zealand (Gamble *et al.*, 1996), were used. The AFC paths in Fig. 9 show that samples with higher $^{87}Sr/^{86}Sr$ and lower $^{206}Pb/^{204}Pb$, $^{207}Pb/^{204}Pb$, Nb/U and Nb/Rb values may be explained by assimilation of arc sediments concurrent with fractional crystallization of $\leq 30\%$ $(1 - F)$.

Mantle metasomatism

It has long been proposed that metasomatic enrichment of the upper mantle by hydrous- or carbonate-rich fluids

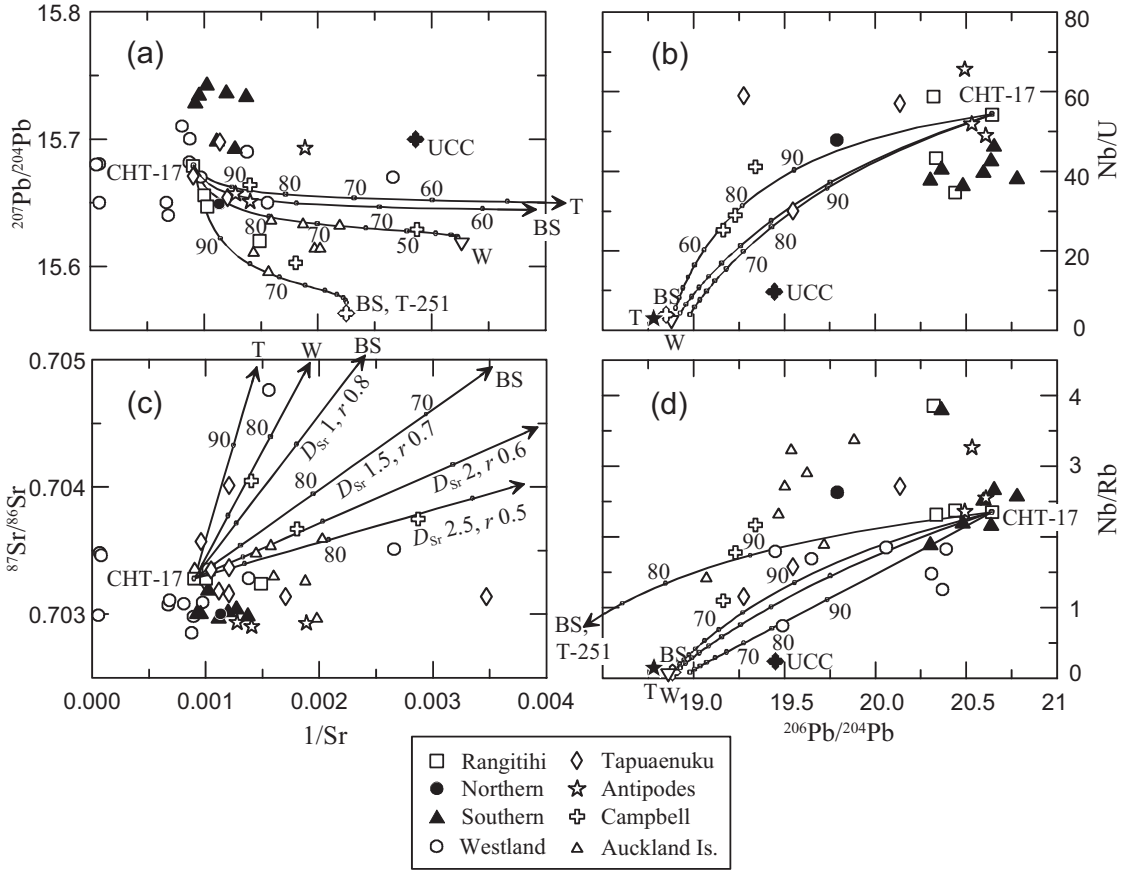

Fig. 9. Variation of $^{207}Pb/^{206}Pb$ and $^{87}Sr/^{86}Sr$ ratios against 1/Sr (a and c) and Nb/U and Nb/Rb against $^{206}Pb/^{204}Pb$ (b and d) for mafic rocks from southern New Zealand. The calculated assimilation–fractional crystallization (AFC) curves use a starting composition of tephrite (CHT-17)—a derivative of 54% closed-system fractional crystallization of basanite sample CHT-20 (refer to text for the specific minerals fractionated). In (a), (b) and (d) all AFC models (DePaolo, 1981) assume a rate of assimilation to fractional crystallization (r) of 0·8; bulk distribution coefficients (D) used are: $D_{Sr} = 1{\cdot}0$, $D_{Nb} = 0{\cdot}2$, and D_{Rb}, D_{Pb} and $D_U = 0{\cdot}1$. Potential assimilants are Torlesse (T) and Waipapa (W) Terrane metasediments (Graham & Mortimer, 1992; Graham *et al.*, 1992) and modern near-trench bulk sediments (BS) collected from the Kermadec–Hikurangi margin (Gamble *et al.*, 1996; BS refers to sediment sample N17/30 unless otherwise indicated). Also shown is average upper continental crust (UCC) from Rudnick & Fountain (1995). (c) D_{Sr} and r values for the assimilation of bulk sediments (BS) by tephrite are indicated. Samples and symbols are the same as in Fig. 8. Numbers along AFC curves denote the per cent fraction of liquid remaining.

or low-volume partial melts may be a necessary precursor to alkaline magmatism (Lloyd & Bailey, 1975; Sun & Hanson, 1975; Wass & Rodgers, 1980) and studies of alkaline rocks from New Zealand support this assertion (Gamble *et al.*, 1986; Barreiro & Cooper, 1987; Weaver & Smith, 1989; Baker *et al.*, 1994; Cook *et al.*, 2005). Alkalis (e.g. K, Rb, Ba) and water are stored within metasomatized upper mantle in amphibole and phlogopite and are retained in these minerals relative to anhydrous minerals during melting (Adam *et al.*, 1993; Dalpé & Baker, 1994; LaTourrette *et al.*, 1995). This effect is displayed prominently by negative K-anomalies on primitive mantle-normalized multi-element plots (Fig. 5). The trace element patterns of other New Zealand mafic alkaline rocks also show negative K-anomalies (Gamble *et al.*, 1986; Weaver & Smith, 1989), suggesting that this is a widespread characteristic of the mantle source (Gamble *et al.*, 1986).

In an effort to constrain mantle source compositions and the role of hydrous phases during melt generation we use the inversion technique described by Hart *et al.* (1997) for modal batch partial melting. Source models are based on the regression of two dominant data arrays observed on reciprocal plots (Fig. 10). The first model consists of the inversion of the entire filtered dataset that includes basalts from each age-delimited suite on Chatham Island and basalts from Antipodes Island (Fig. 10a). The second model is based solely on the regression of the Cretaceous Southern Volcanics from Chatham Island (Fig. 10b). The results of these calculations are summarized in Table 5 and are shown in Fig. 11. The normalized trace element patterns for the two modeled sources are roughly parallel and are both enriched in highly incompatible elements and depleted in heavy REE (HREE) relative to primitive upper mantle (McDonough & Sun, 1995). Also, both patterns show pronounced negative Pb and positive Ti

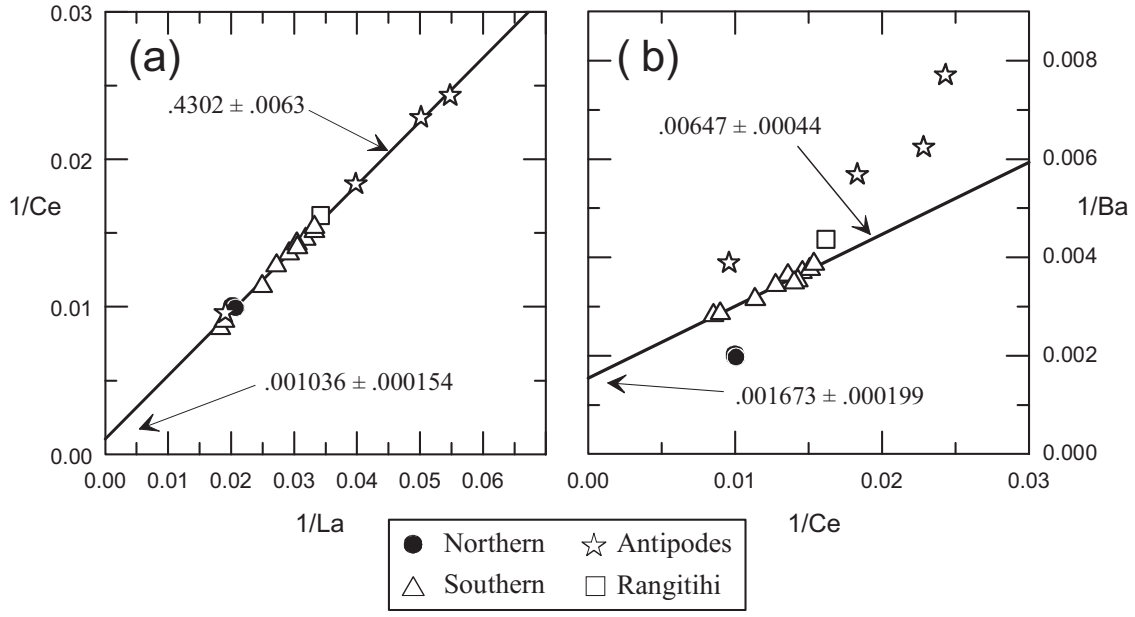

Fig. 10. Representative reciprocal plots of (a) Ce–La and (b) Ba–Ce for Antipodes and Chatham Island basalts. Regression lines show slope and intercepts with corresponding 2σ errors. Samples that were not included in the inversions were those that have been significantly fractionated (MgO ≤6 wt %, Table 2) or possibly contaminated by crust (Campbell Island samples OU39737 and OU39796). Of the remaining samples; CHT-5, -8 and -16 were eliminated because they are considered to represent derivatives of parental magma CHT-20 by fractional crystallization (the Rangitihi Volcanics lineage shown in Fig. 4 and discussed in the text), and CHT-9 and -18 were excluded because, along with some of the other samples from the Northern Volcanic suite, they show strong linear correlations between LOI and elements such as Sr, Rb and Ba, indicating secondary alteration. The remaining 17 samples were corrected for olivine fractionation before they were linearly regressed. In (a) the entire filtered dataset is regressed. In (b) the Southern Volcanic suite is regressed.

anomalies. The models differ most significantly with respect to absolute concentration of LILE (Rb, Ba, Th, U, and K) and HFSE (Zr and Hf). The composition derived for the source of the Southern Volcanics is considered to be homogeneous, consistent with their relatively restricted age (~84–85 Ma; Table 3), limited geographical extent (Fig. 2) and similar petrological characteristics (Figs 4–6). The model composition derived from the entire dataset must, therefore, represent a combined signature that includes a less enriched component.

We believe that some of the compositional disparity between the two models reflects differences in source mineralogy. As discussed previously, amphibole is an important host for K ($K_D^{amp/melt}$ 1·36; Dalpé & Baker, 1994) whereas Rb and Ba are compatible in phlogopite ($K_D^{phl/melt}$ 5·8 and 2·9, respectively; Adam *et al.*, 1993). Modal variations in the melt source of ±3% or less of amphibole and phlogopite, with their proportions set at ~4:1, can adequately account for the differences in K and Ba concentrations between the two models, with the Southern Volcanics source containing a higher percentage of both minerals. The difference in Rb content between the two models is not well matched and would require a higher bulk proportion of phlogopite. The source estimates are based on simple addition using the compositions of vein minerals in peridotites reported by Ionov & Hofmann (1995) and Zanetti *et al.* (1996). If addition of amphibole and phlogopite to the melt source occurs at the expense of clinopyroxene, either by vein–wall-rock interaction or reactive porous flow, then the source may become depleted in Th and U (Schmidt *et al.*, 1999; Tiepolo *et al.*, 2000) relative to neighboring elements (Ba, Nb, Ta and K) on multi-element plots (Fig. 11). The addition of amphibole and phlogopite may also contribute to Ti enrichment, although other Ti-rich phases (e.g. ilmenite and rutile) are known to occur in significant modal abundance in some metasomatized peridotites (Haggerty, 1987; Ionov *et al.*, 1999).

The difference in Zr and Hf concentrations between the models cannot be explained by the simple addition of hydrous phases. However, van Achterbergh *et al.* (2001) documented progressive modal metasomatism in natural peridotites by the reactive replacement of garnet and orthopyroxene by clinopyroxene and phlogopite (± Cr-spinel) accompanied by enrichment in Sr, Na, K, light REE (LREE) and high field strength elements (HFSE; Ti, Zr and Nb) and depletion in Y and HREE. The presence of garnet in the melt sources for New Zealand basalts can be inferred from high Zr/Hf (38–47) and Zr/Yb (120–220) values (see van Westrenen *et al.*, 2001) and moderately steep mantle-normalized trace element patterns (La_N/Yb_N 12–28)

Table 5: Source concentrations for Antipodes and Chatham Island basalts

Element	ANT + CHT Co (ppm)	±2σ	Southern Co (ppm)	±2σ	PUM (ppm)	ANT + CHT Co/PUM	Southern Co/PUM
Cs	0·00453	0·00110	0·00609	0·00217	0·021	0·22	0·29
Rb	0·453	0·120	1·527	0·472	0·6	0·76	2·55
Ba	10·64	1·93	29·65	4·02	6·6	1·61	4·49
Th	0·1155	0·0512	0·2090	0·0793	0·0795	1·45	2·63
U	0·0278	0·0045	0·0632	0·0161	0·0203	1·37	3·11
Nb	1·909	0·308	2·853	0·597	0·658	2·90	4·34
Ta	0·1435	0·0155	0·2055	0·0232	0·037	3·88	5·56
K	282·4	58·0	1149·3	293·8	240	1·18	4·79
La	1·476	0·191	2·055	0·349	0·648	2·28	3·17
Ce	3·354	0·101	4·575	0·202	1·675	2·00	2·73
Pb	0·079	0·022	0·141	0·042	0·15	0·53	0·94
Nd	1·331	0·299	2·172	0·272	1·25	1·06	1·74
Sr	28·59	4·96	42·94	8·81	19·9	1·44	2·16
P	87·6	22·9	181·2	38·3	90	0·97	2·01
Zr	9·51	1·05	20·25	4·74	10·5	0·91	1·93
Hf	0·2733	0·0861	0·5311	0·0752	0·283	0·97	1·88
Sm	0·3637	0·0785	0·5288	0·1016	0·406	0·90	1·30
Eu	0·0974	0·0097	0·1739	0·0316	0·154	0·63	1·13
Ti	1901·0	866·7	2713·4	1476·9	1205	1·58	2·25
Tb	0·0490	0·0164	0·0719	0·0174	0·099	0·50	0·73
Y	1·608	0·259	2·158	0·415	4·3	0·37	0·50
Yb	0·1466	—	0·1466	—	0·441	0·33	0·33
Lu	—	—	0·02092	0·00742	0·0675	—	0·31
$^{87}Rb/^{86}Sr$	0·046		0·103		0·087		
$^{147}Sm/^{144}Nd$	0·166		0·148		0·197		
$^{238}U/^{204}Pb$	22·184		28·294		8·536		
$^{232}Th/^{204}Pb$	95·263		96·732		34·545		
$^{232}Th/^{238}U$	4·3		3·4		4·0		

Primitive upper mantle (PUM) values from McDonough & Sun (1995).

(Fig. 6). The subtle negative Zr–Hf anomalies on mantle-normalized plots (Fig. 5) also imply garnet control during melting ($D^{garnet/melt}$ Zr > Hf ≈ Sm ≫ Sr; Hauri *et al.*, 1994).

The origin of the negative Pb anomalies in Fig. 11 is less clear. Negative Pb anomalies are present in the trace element patterns of all of the basalts (Fig. 5) along with most OIB when normalized to a primitive mantle Ce/Pb value of 11. This may indicate that upper mantle sources are deficient in Pb relative to primitive mantle or that Pb is retained in the mantle by sulfide during melting (Salters et al., 2002; Hart et al., 2005). Alternatively, experimental results indicate that Pb, along with K and Rb, is partitioned into aqueous fluids relative to silicate melts and, therefore, may be fractionated from elements with lower $D^{fluid/melt}$ (e.g. Sr, Nb, Th, U) during mantle metasomatism (Brenan *et al.*, 1995; Keppler, 1996). Based on mineral–fluid partition coefficients it has also been suggested that dehydration of amphibole-rich peridotite could produce a residual source that is depleted in Pb and Rb relative to U, Th, Nb and Sr (Brenan *et al.*, 1995; Stein *et al.*, 1997). The characteristic negative Pb anomalies of the basalts (Fig. 5) may therefore reflect Pb loss during partial dehydration of metasomatized mantle.

Timing of metasomatism

The source metasomatism recorded by the alkaline rocks and mantle xenoliths extends to continental areas outside of New Zealand. During the Paleozoic and Mesozoic the

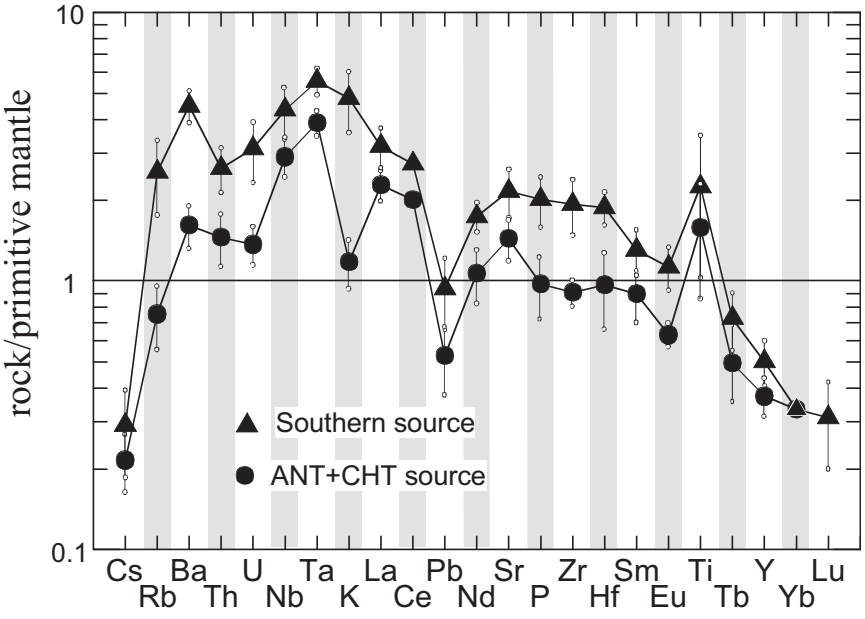

Fig. 11. Model source concentrations for the Southern Volcanic suite and the combined Chatham Island–Antipodes Island dataset normalized to the primitive mantle (PM) values of McDonough & Sun (1995). The source compositions were calculated using the inversion method described by Hart *et al.* (1997) for modal batch melting. Both inversions are based on $Yb_o = 0{\cdot}147$ ($^1/_3$ PM) and the error bars, calculated from errors on regression line slopes and intercepts (e.g. Fig. 10), are plotted at $\pm 2\sigma$. For Ce, the error is within the size of the symbol.

continental blocks of New Zealand were part of the eastern margin of Gondwanaland, juxtaposed to southeastern Australia, Tasmania, and the Victoria Land and Marie Byrd Land provinces of present-day West Antarctica (Lawver *et al.*, 1992; DiVenere *et al.*, 1994; Sutherland, 1999). In each of these areas metasomatized mantle sources for Cenozoic alkaline magmas have been proposed (Hart *et al.*, 1997; Zhang & O'Reilly, 1997; Orlando *et al.*, 2000; Panter *et al.*, 2000*a*; Rocchi *et al.*, 2002; Handler *et al.*, 2003). Estimates for the timing of metasomatism are highly variable, but most suggest that enrichment took place some 100–400 Myr before the mid-Cretaceous break-up of New Zealand from Antarctica.

Depth and location of melting

An estimate of the pressure (depth) of melting for the source of the Chatham and Antipodes basalts can be made using the algorithms derived by Herzberg & Zhang (1996). Our calculations using filtered data corrected for olivine fractionation yield average pressures of ~4·1 GPa (FeO), ~4·4 GPa (MgO), >3·4 GPa (CaO), ~3·9 GPa (Al_2O_3) and >5·2 GPa (Na_2O) for basalts from Chatham Island and ~5·3, ~5·5, >5·1, ~4·3 and >3·1 GPa for basalts from Antipodes Island. The results suggest that melt-equilibration occurred at a greater depth beneath Antipodes Island than Chatham Island; ~160 km vs ~120–130 km based on the MgO and FeO contents. The pressures calculated for each of the three major episodes of volcanism on Chatham Island indicate that the depth of melting has not varied significantly (±0·15 GPa) over a period of ~80 Myr. These results are broadly comparable with depths of melting estimated by Hart *et al.* (1997) for alkaline basalts from the Hobbs Coast, Marie Byrd Land (~110–140 km) using the same Herzberg–Zhang equations, and those of Huang *et al.* (1997) for alkaline basalts from the North Island of New Zealand (~80–140 km) using the experimental data of Hirose & Kushiro (1993).

Pressure estimates and evidence for residual hydrous potassic minerals place important limits on the thermal regime of the melt sources. Experimental studies show that the temperature and pressure stability limits of amphiboles vary with composition. Pargasitic amphibole is stable at temperatures <1100°C at pressures of ~3 GPa (Mengel & Green, 1986; Niida & Green, 1999), whereas K-richterite is stable to higher temperatures (~1200–1250°C) at higher pressures (3–5 GPa, Foley, 1991; Trønnes, 2002). At these pressures the delimited temperature requires a lithospheric source (see Class & Goldstein, 1997; LeRoex *et al.*, 2001). Only synthetic F-rich amphiboles (Foley, 1991) are stable at temperatures that exist at the top of the asthenosphere (~1300°C, McKenzie & Bickle, 1988) but they have not been identified in natural samples (Class & Goldstein, 1997).

Shear-wave velocity models consistently show that the regions of alkaline magmatism from eastern Australia to

New Zealand and West Antarctica are characterized by slow velocity anomalies restricted to a zone between ~60 and 200 km depth (see Finn *et al.*, 2005, fig. 4). Lithospheric thickness estimates of 100–150 km based on elastic models and seismic anisotropy data from Australia (Debayle & Kennett, 2000; Simons *et al.*, 2003) and New Zealand (Scherwath *et al.*, 2002) and scattered broad-band seismometer data from West Antarctica (Winberry & Anandakrishnan, 2003), suggest that part of the observed low-velocity zones (<~100–150 km depth) beneath the continental areas of the SW Pacific (see Finn *et al.*, 2005, fig. 4) reflect melt or volatile sources within the lithosphere and not in the asthenosphere (Finn *et al.*, 2005). A dominantly lithospheric source for volcanism is also consistent with the fact that over the last ~85 Myr, the Chatham Islands have drifted nearly 3000 km north (~65°S to ~44°S) on the Chatham Rise–Campbell Plateau block of Zealandia (Fig. 12) without major changes in source composition or depth of melting (~120–130 km).

Origin of metasomatism and implications for HIMU signatures

The strong HIMU isotopic signature (defined here as $^{206}Pb/^{204}Pb$ >20·5, $^{87}Sr/^{86}Sr$ ~0·703) of basalts from the Antipodes and Chatham Islands, along with other mafic igneous rocks from the South Island, New Zealand (Figs 1 and 8), suggest the widespread occurrence of a pre-Cenozoic HIMU mantle component within the New Zealand lithosphere. Basalts with an equally strong HIMU character are also found in Marie Byrd Land (Hart *et al.*, 1997; Panter *et al.*, 2000*a*) and their melt sources, along with sources for other alkaline rocks with elevated $^{206}Pb/^{204}Pb$ ratios (≥19·5) found throughout the SW Pacific (Fig. 12), have been related to a common origin that pre-dates the Late Cretaceous break-up of the eastern margin of Gondwanaland. Previous studies called upon sources produced by mantle plume activity originating in Mesozoic times (Lanyon *et al.*, 1993; Weaver *et al.*, 1994; Rocholl *et al.*, 1995; Hart *et al.*, 1997) or pre-Cenozoic sources developed from metasomatized continental lithosphere (Rocchi *et al.*, 2002; Cook *et al.*, 2005; Finn *et al.*, 2005) or a combination of both (Panter *et al.*, 2000*a*). A strong case against active mantle plumes in the Cenozoic is based on geological and geophysical evidence that has been thoroughly reviewed and discussed by Finn *et al.* (2005). We will not reiterate these arguments and will limit our discussion to pre-Cenozoic scenarios for metasomatism and the origin of the HIMU component in the SW Pacific.

Considering the geochemical and geophysical evidence presented above, we propose that the HIMU source (1) resides within the subcontinental lithosphere and (2) was produced by interaction of the lithosphere with metasomatic fluids and melts. The case for a lithospheric source for the HIMU magmatism is underscored by the fact that the highest $^{206}Pb/^{204}Pb$ ratios (>20–20·5) are measured only in continental basalts, whereas basalts from nearby ocean islands (Balleny, Scott, Peter I) and crust (Macquarie Island) all have consistently lower ratios (19·0–19·8; Fig. 12a). Indeed, a lithospheric mantle source for the HIMU magmatism has already been proposed, but as plume-derived proto-lithosphere that was introduced and 'stagnated' beneath Gondwanaland (Rocholl *et al.*, 1995; Hart *et al.*, 1997; Panter *et al.*, 2000*a*). With regard to our second assertion that the HIMU signature was generated by the evolution of metasomatic agents, we consider our findings, along with those of others (e.g. Gamble *et al.*, 1986; Baker *et al.*, 1994), to have firmly established the occurrence of residual K-rich hydrous minerals in the melt sources for HIMU-like alkaline magmas in southern New Zealand. However, the temporal relationship between the HIMU component and the metasomatism has not been discussed. It has been recognized that in Marie Byrd Land the strong HIMU component is preferentially sampled by low-degree (≤2%) partial melts (Hart *et al.*, 1997; Panter *et al.*, 2000*a*). This is indicated by the negative correlation between K/K* and Pb/Pb* and $^{206}Pb/^{204}Pb$ values; i.e. lower K/K* and Pb/Pb* values [values <1 appear as negative K- and Pb-anomalies on primitive mantle normalized multi-element plots (Fig. 5)] represent smaller degrees of melting when K- and Pb-compatible minerals are retained in the residuum. Similar correlations for the New Zealand data strengthen this interpretation (Fig. 13b and c), although, as discussed above, low relative Pb contents may be a relic of the source composition (Fig. 11) and not solely a product of partial melting. Nevertheless, it follows that melting localized around veins containing minerals with lower solidus temperatures (amphibole, mica, apatite, clinopyroxene) will consume a greater proportion of these minerals relative to more refractory assemblages (olivine and orthopyroxene) in the surrounding peridotites. This establishes a link between metasomatism and the strong HIMU signature. *In situ* storage of modified lithosphere over a sufficient time-span before reactivation and further fractionation by vein-plus-wall-rock melting mechanisms (see Foley, 1992) may explain some of the range in isotope compositions for SW Pacific basalts (see Finn *et al.*, 2005, Fig. 7) and the variable enrichment of their melt sources [Fig. 11; also see Hart *et al.* (1997, fig. 8) and Rocchi *et al.* (2002, fig. 10)].

Ancient plumes and metasomatism

Amphibole and phlogopite may have been introduced into the Gondwanaland lithosphere by infiltrating melts or fluids derived from rising mantle plume material.

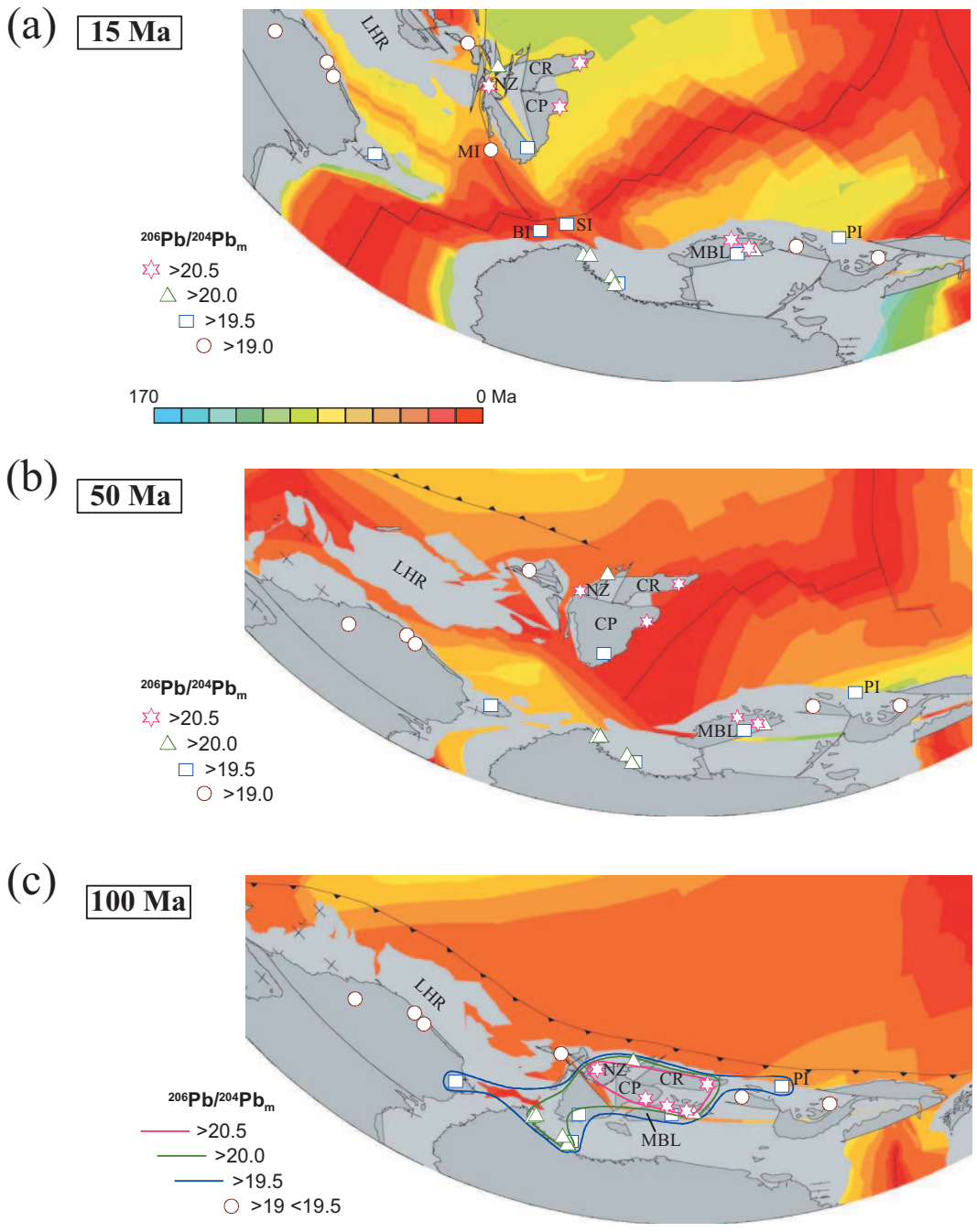

Fig. 12. Plate reconstructions of the SW Pacific and the proto-Pacific margin of Gondwanaland (modified from Finn *et al.*, 2005). Colors indicate age of ocean floor (Müller *et al.*, 1993). (a) A 15 Ma reconstruction overlain with locations of late Cretaceous and Cenozoic alkaline mafic rocks with measured $^{206}Pb/^{204}Pb$ ratios >19·0. NZ, New Zealand; CR, Chatham Rise; CP, Campbell Plateau; MI, Macquarie Island; LHR, Lord Howe Rise; BI, Balleny Islands; SI, Scott Island; MBL, Marie Byrd Land; PI, Peter I. (b) A 50 Ma reconstruction. (c) A 100 Ma reconstruction with $^{206}Pb/^{204}Pb$ ratios contoured at 0·5 intervals. Sources for Pb isotopes listed in Fig. 8 with additional sources for Auckland basalts (NZ) from Huang *et al.* (1997) and Cook *et al.* (2005); Tasmania basalts from Lanyon *et al.* (1993); SE Australian basalts from Ewart *et al.* (1988) and Zhang *et al.* (1999); Marie Byrd Land (Antarctica) basalts from Hart *et al.* (1997) and Panter *et al.* (1997, 2000*a*); Victoria Land (Antarctica) basalts from Sun & Hanson (1975), Rocholl *et al.* (1995) and Panter *et al.* (2003); Antarctic Peninsula basalts from Hole *et al.* (1993).

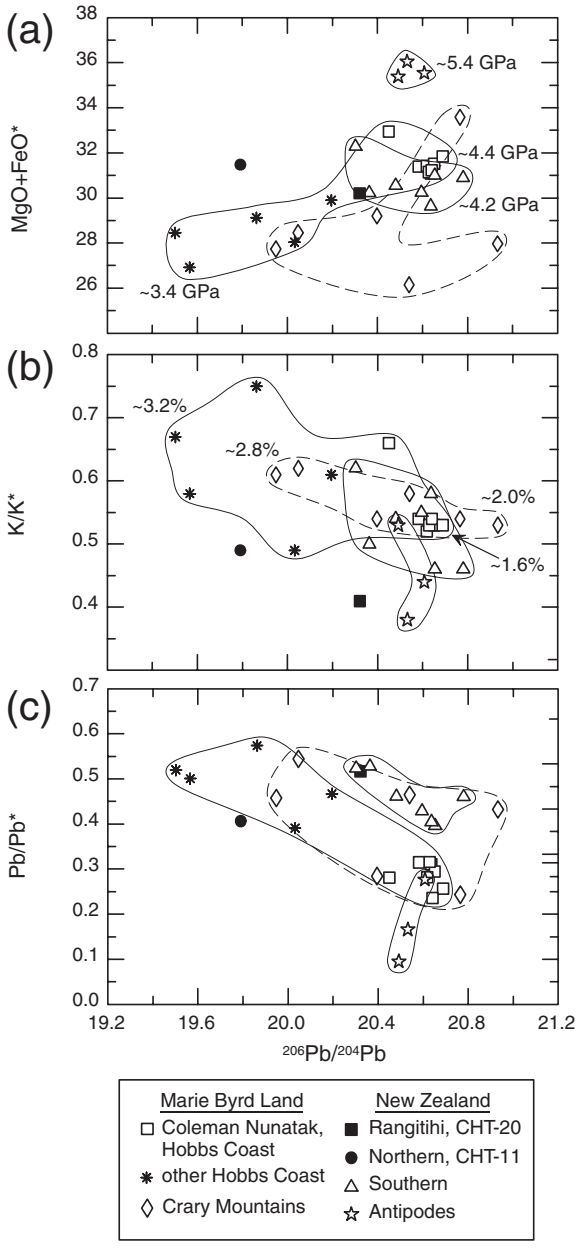

Fig. 13. Variation of (a) MgO + FeO*, (b) K/K* and (c) Pb/Pb* vs $^{206}Pb/^{204}Pb$ for basalts from New Zealand (this study) and Marie Byrd Land (Hobbs Coast, Hart *et al.*, 1997; Crary Mountains, Panter *et al.*, 2000*a*). K/K* and Pb/Pb* values determined by $K_{PM}/\sqrt{(Ta_{PM} \times La_{PM})}$ and $Pb_{PM}/\sqrt{(Ce_{PM} \times Nd_{PM})}$, respectively. In (a) labeled values are average melt equilibration pressures (in GPa) determined using the algorithms of Herzberg & Zhang (1996) for MgO and FeO* (total iron as FeO). In (b) labeled values represent per cent partial melt determined by Hart *et al.* (1997) for the Hobbs Coast and Panter *et al.* (2000*a*) for the Crary Mountains. All of the data have been corrected for olivine fractionation.

A possible pre-Cenozoic plume has been associated with the fragmentation of the eastern margin of Gondwanaland in the mid–late Cretaceous (Lanyon *et al.*, 1993; Weaver *et al.*, 1994; Storey *et al.*, 1999). Weaver *et al.* (1994) placed the axis of their proposed 2000 km diameter plume head at the reconstructed boundary between New Zealand and Marie Byrd Land, which intersects the region delimited by the highest $^{206}Pb/^{204}Pb$ values (>20·5) in Fig. 12c. Arguments against a late Cretaceous plume are based on the lack of large-scale regional uplift (LeMasurier & Landis, 1996), the unrealistically short time interval (5–10 Myr) for the switch from subduction-driven magmatism to plume-driven magmatism (Dalziel *et al.*, 2000; Mukasa & Dalziel, 2000) and the much lower than expected magma production rates relative to plume-related large flood basalt provinces (Finn *et al.*, 2005). An earlier plume event may have been responsible for the magmatism that produced the Jurassic Karoo–Ferrar large igneous province (Storey, 1995; Storey & Kyle, 1997; Dalziel *et al.*, 2000; Storey *et al.*, 2001). However, the geochemical character of the mantle source of the Ferrar magmatism is unresolved (Kyle *et al.*, 1983; Hergt *et al.*, 1991; Molzahn *et al.*, 1996; Demarchi *et al.*, 2001; Hergt & Brauns, 2001). Hart *et al.* (1997) suggested that a large, two-component (HIMU + FOZO), mantle plume metasomatized and enriched the Gondwanaland lithosphere prior to break-up. In this model, the rising plume head, weakened by thermal entrainment of ambient mantle, was flattened and flowed over a vast region beneath the Gondwanaland lithosphere, with little, if any, associated volcanism. The plume and metasomatically enriched lithospheric mantle material was then preserved to form a young and geochemically stratified component of the sub-Gondwanaland lithosphere (compare with the fossil plume model of Stein & Hofmann, 1992).

Geochemical studies that favor ancient mantle plumes as sources for continental alkaline magmatism in the SW Pacific, however, do not adequately account for the seemingly unavoidable physical and chemical interaction between a rising plume head and subduction that was active along the proto-Pacific margin of Gondwanaland between ~500 and 100 Ma (Bradshaw, 1989; Borg & DePaolo, 1991; Elliot, 1991; Lawver *et al.*, 1992). Dalziel *et al.* (2000) presented a model in which the impingement of a plume head beneath subducted oceanic lithosphere in the late Paleozoic flattened the angle of slab descent and contributed to the early Mesozoic Gondwanide orogeny. The thermal and mechanical breakthrough of the slab by the plume is considered to have taken place some 30–60 Myr later and was followed by Karoo–Ferrar magmatism. Subduction was re-established along the proto-Pacific margin soon after the slab was penetrated. Although Dalziel *et al.* (2000) did not discuss the geochemical implications of their model, they do offer a plausible scenario for plume–lithosphere interaction beneath a region that would later produce alkaline magmatism.

Subduction and metasomatism

The most important mechanism responsible for the introduction of hydrous and CO_2-rich melts and fluids back into the mantle is the subduction of oceanic lithosphere, including hydrothermally altered upper oceanic crust (± sediments). There are several lines of evidence to suggest that the metasomatized mantle sources for continental alkaline magmatism in the SW Pacific may be linked to subduction with, or without, plume influence. First, the calculated chronology of metasomatic enrichment estimated from basalts and mantle xenoliths coincides with subduction along the eastern margin of Gondwanaland (~500–100 Ma). Second, if it is accepted that the products of metasomatism reside within the subcontinental mantle lithosphere and were in place before Gondwanaland break-up, then the sources of the alkaline magmas would be inboard of and roughly parallel to the subduction zone at ≥100 Ma (Fig. 12c). Additionally, it is important to note that the regions with the longest history of subduction correspond to sources having the strongest HIMU signatures (highest $^{206}Pb/^{204}Pb$ values, Fig. 12).

However, if the metasomatism is subduction-related, then why do the magmas lack the classic subduction fingerprint (high LILE/HFSE ratios, e.g. Ba/Nb, Rb/Nb, etc.) recorded in island arc and active continental margin magmas? We suggest that the alkaline magmas were generated, in part, within a region of the lithosphere that had been metasomatized (veined) by subduction-related melts or fluids but that did not contain what would be regarded as a typical arc signature. On the basis of the concept of chromatographic separation of trace elements in mantle environments (e.g. Navon & Stolper, 1987; Hawkesworth *et al.*, 1993), Ionov & Hofmann (1995) and Stein *et al.* (1997) have developed subduction-related metasomatic models to explain the retention of Nb and Ta in hydrous minerals within the lowermost portion of the mantle wedge above a devolatilizing slab [Fig. 14a (1)]. In these models, slab fluids enriched in incompatible elements migrate upwards into the mantle wedge. Some of the fluids reach the melt-generation zone above the wet solidus for peridotite [the source for arc magmas; Fig. 14a (2)] while others react metasomatically with the surrounding peridotite near the cool base of the wedge to form Nb-rich amphiboles and micas in veins. This enriched region of the mantle is transported by buoyancy-induced convective flow (Davies & Stevenson, 1992) to areas above the *P–T* stability limit of amphibole where it becomes partially dehydrated [Fig. 14a (3 and 4)]. The post-metasomatic partial dehydration of the mantle causes it to become depleted in the hydrophile elements Rb and Pb relative to more magmaphile elements Th, U, Nb and Sr (Brenan *et al.*, 1995; Keppler, 1996), producing high Th–U/Pb, low Rb/Sr and Rb/Nb, and relatively unmodified Sm/Nd ratios. If this mantle region is then isolated near the base of the lithosphere [Fig. 14a (5)] for a sufficient period of time it may develop isotopic signatures that are similar to mantle sources of HIMU-type ocean island basalts.

Cause of Cretaceous–Cenozoic magmatism

The most likely trigger for the Cretaceous alkaline magmatism in New Zealand was extension and lithospheric thinning associated with the break-up of New Zealand from Antarctica, which was in turn a response to the collision (Bradshaw, 1989) or near collision (Luyendyk, 1995) of the Pacific–Phoenix ridge with the eastern margin of Gondwanaland. According to Finn *et al.* (2005), most of the Cenozoic magmatism in the SW Pacific was a response to the sudden detachment and sinking of subducted slabs into the lower mantle during the late Cretaceous. This may have caused vertical and lateral flow of warm asthenosphere into 'thin-spots' at the base of the lithosphere (see King & Anderson, 1995), catalyzing melting of amphibole/phlogopite-rich veins (Fig. 14b). Also, mid-Cenozoic to active extension in the southern Ross Sea (Cape Roberts Science Team, 1998, 1999, 2000; Willis *et al.*, 2004) and dextral transtension along faults in northern Victoria Land (Rocchi *et al.*, 2002; Di Vincenzo *et al.*, 2004) may have caused local decompression melting in these areas.

CONCLUSIONS

Continental intraplate mafic magmatism in southern New Zealand consists of relatively small volume melts erupted from widely distributed centers located on the South Island and offshore on the submerged continental crust of the Chatham Rise and Campbell Plateau. We have presented geochemical data on mafic rocks from three islands; Campbell, Antipodes and Chatham, to elucidate the magmatic history, mantle sources and fundamental cause of alkaline volcanism in this region, as well as in adjacent continental areas of the SW Pacific. Our main conclusions are as follows.

(1) Volcanism on Chatham Island produced subaerial lavas and associated pyroclastic rocks in three distinct eruptive episodes: late Cretaceous (85–82 Ma), late Eocene (41–35 Ma) and Miocene–Pliocene (~5 Ma). Dating by the $^{40}Ar/^{39}Ar$ method modifies earlier interpretations based on K–Ar dates (Grindley *et al.*, 1977); most notably, that the Cretaceous basalts are significantly older than previously thought.

(2) Fractionation-corrected whole-rock compositions from all three islands display similar trace element characteristics that have OIB-like trace element ratios (e.g. Ce/Pb 28–36, Nb/U 34–36, Ba/Nb 4–7, La_N/Yb_N 12–28) and prominent negative K- and Pb-anomalies on primitive mantle-normalized multi-element plots. The

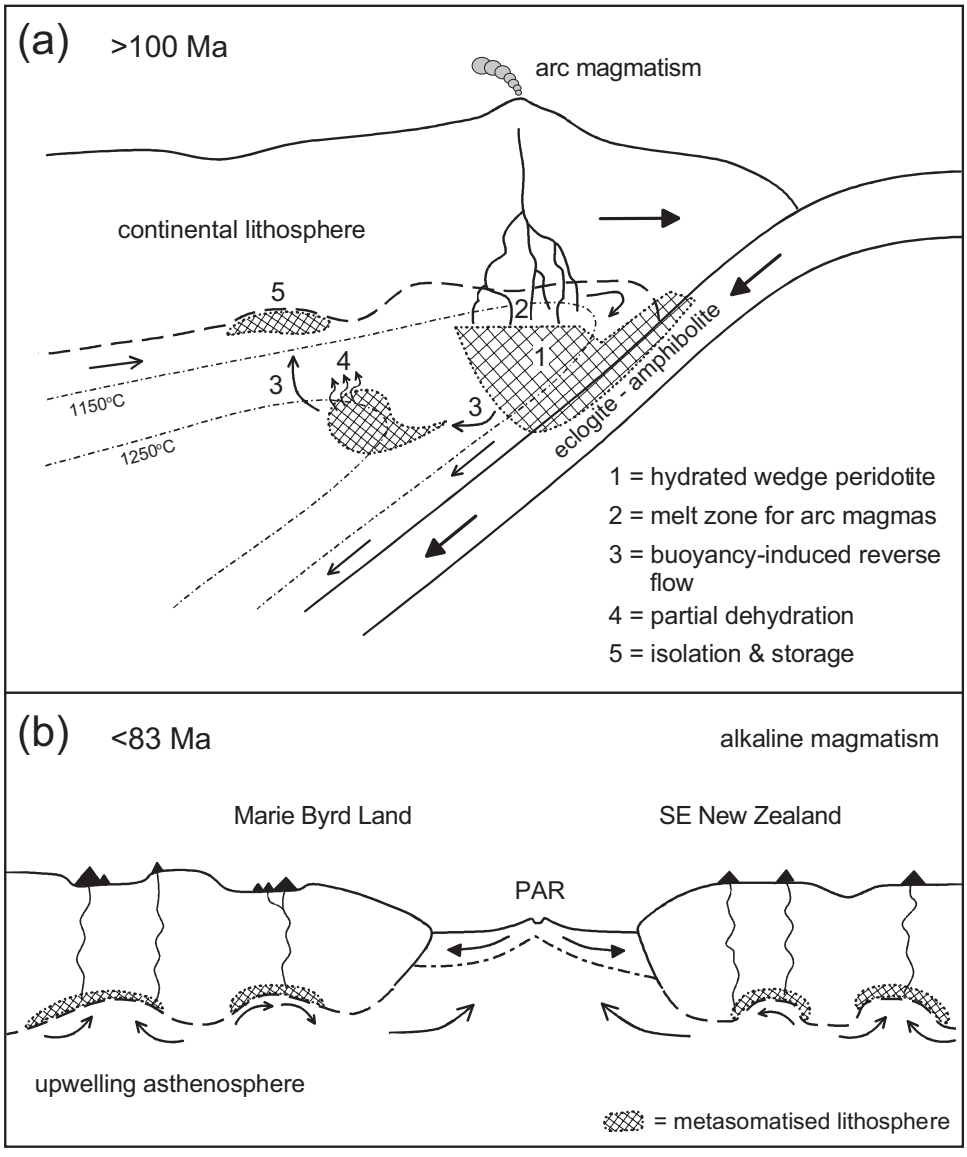

Fig. 14. Schematic illustration of the development of HIMU-like mantle reservoirs by subduction-related metasomatism (a) that may become sources for continental alkaline magmatism in the SW Pacific (b). (a) Model of the active Gondwanaland margin prior to 100 Ma. 1, Hydrated peridotite; incompatible element enriched fluids liberated from progressive dehydration of subducted oceanic crust + sediments migrate into the overlying mantle wedge, react and precipitate Nb-rich amphibole and mica in veins (Ionov & Hofmann, 1995). 2, Melt zone; residual fluids depleted in Nb (and Ta) migrate upward and induce melting above the wet solidus to form arc magmas. 3, Reverse flow; diapirs of hydrated peridotite are decoupled from the descending slab and rise buoyantly (Davies & Stevenson, 1992). 4, Partial dehydration; buoyant diapirs rise through the warmer central portion of the wedge where amphibole becomes unstable. Fluids liberated by this process are enriched in Pb and Rb relative to U, Th and Sr, producing a high U–Th/Pb and low Rb/Sr residuum. 5, Isolation & storage; partially dehydrated, amphibole-rich peridotite stabilizes at the base of the continental lithosphere where it becomes isolated from convective flow. Relatively short-term (≤0·5–0·1 Ga) storage of this mantle may generate HIMU-like sources. (b) Schematic cross-section after Gondwanaland break-up (<83 Ma). The Pacific–Antarctic Ridge (PAR) separates SE New Zealand from the Marie Byrd Land coast. Localized extension and/or upwelling asthenosphere induce melting of metasomatized lithosphere in thin spots to produce alkaline magmas with HIMU-like isotopic signatures. The metasomatism may have been produced by subduction-related processes illustrated in (a) or by plume–lithosphere interaction prior to continental break-up.

basalts show a restricted range in measured isotope ratios and the majority have high $^{206}Pb/^{204}Pb$ (20·3–20·8) and low $^{87}Sr/^{86}Sr$ (∼0·7030) values similar to HIMU OIB. The more radiogenic $^{87}Sr/^{86}Sr$ (>0·7036) rocks from Campbell Island can be explained by the local assimilation of continental crust.

(3) Inversion models for the Antipodes and Chatham islands suggest mantle sources that are enriched in highly

incompatible elements relative to primitive mantle. Chemical heterogeneity, inferred from the models, is associated with modal variations in anhydrous and hydrous (amphibole and mica) minerals within a veined mantle.

(4) Calculated melt equilibration depths of ~160 km (Antipodes) and ~130 km (Chatham), together with estimates from geophysical data and the P–T stability limits of hydrous minerals, suggest that melting occurred primarily within the subcontinental lithospheric mantle. This is also supported by the fact that Chatham Island drifted ~3000 km over 85 Myr without a significant change in source composition or depth of melting.

(5) Metasomatized lithosphere is considered the source for alkaline magmatism in other areas of New Zealand, as well as adjacent continental fragments of Gondwanaland (SE Australia, Tasmania, Victoria Land and Marie Byrd Land). The timing of metasomatism is constrained to between 500 and 100 Ma, coincident with subduction and the distribution of HIMU volcanism.

(6) Metasomatism and enrichment of the uppermost mantle by a mantle plume and subsequent preservation of this material at the base of the Gondwanaland lithosphere prior to break-up may provide the source for the late Cretaceous–Cenozoic alkaline magmatism in the SW Pacific. However, models that ascribe to an ancient plume source must also account for the likely physical and chemical interaction between a rising plume head and subducted oceanic lithosphere.

(7) Metasomatism, enrichment and the source of the strong HIMU signature may be the result of a complex multi-stage chromatographic separation process (see Stein *et al.*, 1997) consisting of: (a) devolatilization of subducted oceanic crust, which enriched the overlying peridotite in incompatible elements (e.g. Th, U, K, Pb, Nb, Sr, Rb, LREE) and deposited K–Nb (Ta)-rich hydrous minerals in veins; (b) buoyant convection and partial dehydration of the veined peridotite, depleting hydrophile elements (e.g. Pb, Rb, ± K) relative to more magmaphile elements (e.g. Th, U, Sr); (c) preservation and storage of what has become a high Th–U/Pb and low Rb/Sr source at the base of the Gondwanaland lithosphere.

(8) The metasomatized lithospheric source was later sampled by low degrees of partial melting triggered by extension-related decompression and/or warm upwelling asthenosphere over the past 100 Myr.

ACKNOWLEDGEMENTS

We would like to thank John Gamble, Steve Weaver, Tony Reay and Douglas Coombs for access to collection of subantarctic island samples in New Zealand; the Tuanui family and Kevin Bliss for their warm hospitality during our stay on Chatham Island; and Ann Beck for her support and assistance in the field. We would also like to thank Mark Kurz for access to the VG-354 facility at WHOI, Nelia Dunbar for microprobe analyses at NMT, Joel Baker for unpublished Tapuaenuku analyses, E. K. Esawi for instruction on the use of his AMPH-CLASS program (Esawi, 2004), and Dietmar Müller for plate reconstructions. Special thanks go to Carol Finn (USGS) for informative discussions from a geophysical perspective. Official reviews by John Gamble, Joel Baker, Richard Wysoczanski and additional comments made by Craig Cook significantly improved the manuscript and are gratefully acknowledged. This study was supported by National Science Foundation Grants OPP-9419686 and OPP-0003702 awarded to K.S.P.

REFERENCES

Adam, J., Green, T. H. & Sie, S. H. (1993). Proton microprobe determined partitioning of Rb, Sr, Ba, Y, Zr, Nb and Ta between experimentally produced amphiboles and silicate melts with variable F content. *Chemical Geology* **109**, 29–49.

Adams, C. J. & Cooper, A. F. (1996). K–Ar age of a lamprophyre dike swarm near Lake Wanaka, west Otago, South Island, New Zealand. *New Zealand Journal of Geology and Geophysics* **39**, 17–23.

Adams, C. J., Morris, P. A. & Beggs, J. M. (1979). Age and correlation of volcanic rocks of Campbell Island and metamorphic basement of the Campbell Plateau, south-west Pacific. *New Zealand Journal of Geology and Geophysics* **22**, 679–691.

Adams, C. J., Seward, D. & Weaver, S. D. (1995). Geochronology of Cretaceous granites and metasedimentary basement on Edward VII Peninsula, Marie Byrd Land, West Antarctica. *Antarctic Science* **7**, 265–276.

Adams, C. J., Campbell, H. J., Graham, I. J. & Mortimer, N. (1998). Torlesse, Waipapa and Caples suspect terranes of New Zealand: integrated studies of their geological history in relation to neighboring terranes. *Episodes* **21**, 135–240.

Baker, J. A., Gamble, J. A. & Graham, I. J. (1994). The age, geology, and geochemistry of the Tapuaenuku Igneous Complex, Marlborough, New Zealand. *New Zealand Journal of Geology and Geophysics* **37**, 249–268.

Baker, J. A., Menzies, M. A., Thirlwall, M. F. & Macpherson, C. G. (1997). Petrogenesis of Quaternary intraplate volcanism, Sana'a, Yemen: plume–lithosphere interaction and polybaric melt hybridization. *Journal of Petrology* **38**, 1359–1390.

Ballentine, C. J., Lee, D.-C. & Halliday, A. N. (1997). Hafnium isotopic studies of the Cameroon line and new HIMU paradoxes. *Chemical Geology* **139**, 111–124.

Barreiro, B. A. & Cooper, A. F. (1987). A Sr, Nd and Pb isotope study of alkaline lamprophyres and related rocks from Westland and Otago, South Island, New Zealand. *Geological Society of America, Special Publications* **215**, 115–125.

Barry, T. L., Saunders, A. D., Kempton, P. D., Windley, B. F., Pringle, M. S., Dorjnamjaa, D. & Saandar, S. (2003). Petrogenesis of Cenozoic basalts from Mongolia: evidence for the role of asthenospheric versus metasomatized lithosphere mantle sources. *Journal of Petrology* **44**, 55–91.

Beggs, J. M. (1993). Depositional and tectonic history of the Great South Basin. In: Ballance, P. F. (ed.) *South Pacific Sedimentary Basins. Sedimentary Basins of the World, 2*. Amsterdam: Elsevier, pp. 93–107.

Beggs, J. M., Challis, G. A. & Cook, R. A. (1990). Basement geology of the Campbell Plateau: implications for correlation of the Campbell magnetic anomaly system. *New Zealand Journal of Geology and Geophysics* **33**, 401–404.

Behrendt, J. C., LeMasurier, W. E. & Cooper, A. K. (1992). The West Antarctic rift system—a propagating rift 'captured' by a mantle plume. In: Yoshida, Y., Kaminuma, K. & Shirashi, K. (eds) *Recent Progress in Antarctic Earth Science*. Tokyo: Terra, pp. 315–322.

Behrendt, J. C., Saltus, R., Damaske, D., McCafferty, Flinn, C. A., Blankenship, D. & Bell, R. E. (1996). Patterns of Late Cenozoic and tectonic activity in the West Antarctic rift system revealed by aeromagnetic surveys. *Tectonics* **15**, 660–676.

Bishop, D. G., Bradshaw, J. D. & Landis, C. A. (1985). Provisional terrane map of South Island, New Zealand. In: Howell, D. G. (ed.) *Tectonostratigraphic Terranes. Circum-Pacific Council for Energy and Mineral Resources, Earth Science Series* **1**, 515–521.

Blusztajn, J. & Hegner, E. (2002). Osmium isotopic systematics of melilitites from the Tertiary Central European Volcanic Province in SW Germany. *Chemical Geology* **189**, 91–103.

Borg, S. G. & DePaolo, D. J. (1991). A tectonic model of the Antarctic Gondwana margin with implications for southeast Australia isotopic and geochemical evidence. *Tectonophysics* **196**, 339–358.

Bradshaw, J. D. (1989). Cretaceous geotectonic patterns in the New Zealand region. *Tectonics* **8**, 803–820.

Bradshaw, J. D., Pankhurst, R. J., Weaver, S. D., Storey, B. C., Muir, R. J. & Ireland, T. R. (1997). New Zealand superterranes recognized in Marie Byrd Land and Thruston Island. In: Ricchi, C. A. (ed.) *The Antarctic Region: Geological Evolution and Processes*. Siena: Terra Antartica, pp. 429–436.

Brenan, J. M., Shaw, H. F., Ryerson, F. J. & Phinney, D. L. (1995). Mineral–aqueous fluid partitioning of trace elements at 900°C and 2·0 GPa: constraints on the trace element chemistry of mantle and deep crustal fluids. *Geochimica et Cosmochimica Acta* **59**, 331–3350.

Campbell, H. J., Andrews, P. B., Beu, A. G., Maxwell, P. A., Edwards, A. R., Laird, M. G., Hornibrok, N. B., Mildenhall, D. C., Watters, W. A., Buckeridge, J. S., Lee, D. E., Strong, C. P., Wilson, G. J. & Hayward, B. W. (1993). *Cretaceous–Cenozoic Geology and Biostratigraphy of the Chatham Islands, New Zealand. Institute of Geological & Nuclear Sciences Monograph* **2**, 269 pp.

Cape Roberts Science Team (1998). Studies from the Cape Roberts Project, Ross Sea, Antarctica—Initial Report on CRP-1. In: Ricci, C. A. (ed.) *Terra Antartica*. Siena: Museo Nazionale dell'Antartide, Siena, pp. 1–187.

Cape Roberts Science Team (1999). Studies from the Cape Roberts Project, Ross Sea, Antarctica—Initial Report on CRP-2/2A. In: Ricci, C. A. (ed.) *Terra Antartica*. Siena: Museo Nazionale dell'Antartide, pp. 1–173.

Cape Roberts Science Team (2000). Studies from the Cape Roberts Project, Ross Sea, Antarctica—Initial Report on CRP-3. In: Ricci, C. A. (ed.) *Terra Antartica*. Siena: Museo Nazionale dell'Antartide, pp. 1–209.

Caroff, M., Maury, R. C., Leterrier, J., Joron, J. L., Cotten, J. & Guille, G. (1993). Trace element behaviour in the alkali basalt–comenditic trachyte series from Mururoa Atoll, French Polynesia. *Lithos* **30**, 1–22.

Class, C. & Goldstein, S. L. (1997). Plume–lithosphere interactions in the ocean basins; constraints from the source mineralogy. *Earth and Planetary Science Letters* **150** (3–4), 245–260.

Cook, C., Briggs, R. M., Smith, I. E. M. & Maas, R. (2005). Petrology and geochemistry of intraplate basalts in the south Auckland volcanic field, New Zealand: evidence for two coeval magma suites from distinct sources. *Journal of Petrology* **46** (3), 473–503.

Coombs, D. S., Cas, R., Kawachi, Y., Landis, C. A., McDonough, W. F. & Reay, A. (1986). Cenozoic volcanism in north, east and central Otago. In: Smith, I. E. M. (ed.) *Late Cenozoic Volcanism in New Zealand*. Wellington: Royal Society of New Zealand, pp. 278–312.

Cullen, D. J. (1969). Quaternary volcanism at the Antipodes Islands: its bearing on structural interpretation of the southwest Pacific. *Journal of Geophysical Research* **74**, 4213–4220.

Dalpé, C. & Baker, D. R. (1994). Partition coefficients for rare-earth elements between calcic amphibole and Ti-rich basanitic glass at 1·5 GPa, 1100°C. *Mineralogical Magazine* **58A**, 207–208.

Dalziel, I. W. D., Lawver, L. A. & Murphy, J. B. (2000). Plumes, orogenesis, and supercontinental fragmentation. *Earth and Planetary Science Letters* **178**, 1–11.

David, K., Schiano, P. & Allègre, C. J. (2000). Assessment of the Zr/Hf fractionation in oceanic basalts and continental materials during petrogenetic processes. *Earth and Planetary Science Letters* **178**, 285–301.

Davies, J. H. & Stevenson, D. J. (1992). Physical model of source region of subduction zone volcanics. *Journal of Geophysical Research* **97**, 2037–2070.

Davy, B. (1993). The Bounty Trough—basement structure influences on sedimentary basin evolution. In: Ballance, P. F. (ed.) *South Pacific Sedimentary Basins. Sedimentary Basins of the World, 2*. Amsterdam: Elsevier, pp. 69–90.

Debayle, E. & Kennett, B. L. N. (2000). Anisotropy in the Australasian upper mantle from Love and Rayleigh waveform inversion. *Earth and Planetary Science Letters* **184** (1), 339–351.

Demarchi, G., Antonini, P., Piccirillo, E. M., Orsi, G., Civetta, L. & D'Antonio, M. (2001). Significance of orthopyroxene and major element constraints on the petrogenesis of Ferrar tholeiites from southern Prince Albert Mountains, Victoria Land, Antarctica. *Contributions to Mineralogy and Petrology* **142**, 127–146.

DePaolo, D. J. (1981). Trace element and isotopic effects of combined wallrock assimilation and fractional crystallization. *Earth and Planetary Science Letters* **53**, 189–202.

DiVenere, V., Kent, D. V. & Dalziel, I. W. D. (1994). Mid-Cretaceous paleomagnetic results from Marie Byrd Land, west Antarctica: a test of post-100 Ma relative motion between east and west Antarctica. *Journal of Geophysical Research* **99**, 15115–15139.

Di Vincenzo, G., Rocchi, S., Rossetti, F. & Storti, F. (2004). $^{40}Ar/^{39}Ar$ dating of pseudotachylytes: the effect of clast-hosted extraneous argon in Cenozoic fault-generated friction melts from the West Antarctic Rift System. *Earth and Planetary Science Letters* **223**, 349–364.

Duggan M. B. & Reay, A. (1986). The Timaru Basalt. *Royal Society of New Zealand Bulletin* **23**, 246–277.

Elliot, D. H. (1991). Triassic–Early Cretaceous evolution of Antarctica. In: Thomson, M. R. A. (ed.) *Geological Evolution of Antarctica*. New York: Cambridge University Press, pp. 541–548.

Esawi, E. K. (2004). AMPH-CLASS: an Excel spreadsheet for the classification and nomenclature of amphiboles based on the 1997 recommendations of the International Mineralogical Association. *Computers and Geosciences* **30**, 753–760.

Ewart, A., Chappell, B. W. & Menzies, M. A. (1988). An overview of the geochemical and isotopic characteristics of the eastern Australian Cainozoic volcanic provinces. *Journal of Petrology, Special Lithosphere Issue*, 225–273.

Finn, C. A., Müller, R. D. & Panter, K. S. (2005). A Cenozoic diffuse alkaline magmatic province in the SW Pacific without rift or plume origin. *Geochemistry, Geophysics, Geosystems*, doi:10.1029/2004GC000723.

Foley, S. (1991). High-pressure stability of the fluor- and hydroxyl-end-members of paragasite and K-richterite. *Geochimica et Cosmochimica Acta* **55**, 2689–2694.

Foley, S. (1992). Vein-plus-wall-rock melting mechanisms in the lithosphere and the origin of potassic alkaline magmas. *Lithos* **28**, 435–453.

Franz, G., Steiner, G., Volker, F., Pudlo, D. & Hammerschmidt, K. (1999). Plume related alkaline magmatism in central Africa—the Meidob Hills (W Sudan). *Chemical Geology* **157**, 27–47.

Gamble, J. A. & Adams, C. J. (1990). Antipodes Islands. In: LeMasurier, W. E. & Thomson, J. W. (eds) *Volcanoes of the Antarctic Plate and Southern Oceans. Antarctic Research Series, American Geophysical Union* **48**, 468–469.

Gamble, J. A., Morris, P. A. & Adams, C. J. (1986). The geology, petrology and geochemistry of Cenozoic volcanic rocks from the Cambell Plateau and Chatham Rise. In: Smith, I. E. M. (ed.) *Late Cenozoic Volcanism in New Zealand. Royal Society of New Zealand Bulletin* **23**, 344–365.

Gamble, J. A., Woodhead, J., Wright, I. & Smith, I. (1996). Basalt and sediment geochemistry and magma petrogenesis in a transect from oceanic island arc to rifted continental margin arc: the Kermadec–Hikurangi margin, SW Pacific. *Journal of Petrology* **37**, 1523–1546.

Godfrey, N. J., Davey, F., Stern, T. A. & Okaya, D. (2001). Crustal structure and thermal anomalies of the Dunedin region, South Island, New Zealand. *Journal of Geophysical Research* **106**, 30835–30848.

Graham, I. J. & Mortimer, N. (1992). Terrane characterization and timing of metamorphism in the Otago Schist, New Zealand, using Rb–Sr and K–Ar geochronology. *New Zealand Journal of Geology and Geophysics* **35**, 391–401.

Graham, I. J., Gulson, B. L., Hedenquist, J. W. & Mizon, K. (1992). Petrogenesis of Late Cenozoic volcanic rocks from the Taupo Volcanic Zone, New Zealand, in the light of new lead isotope data. *Geochimica et Cosmochimica Acta* **56**, 2797–2819.

Grapes, R. H. (1975). Petrology of the Blue Mountain Complex, Marlborough, New Zealand. *Journal of Petrology* **16**, 371–428.

Grindley, G. W., Adams, C. J. D., Lumb, J. T. & Watters, W. A. (1977). Paleomagnetism, K–Ar dating and tectonic interpretation of Upper Cretaceous and Cenozoic volcanic rocks of the Chatham Islands, New Zealand. *New Zealand Journal of Geology and Geophysics* **20**, 425–467.

Haggerty, S. E. (1987). Metasomatic mineral titanites in upper mantle xenoliths. In: Nixon, P. H. (ed.) *Mantle Xenoliths*. Chichester: Wiley, pp. 671–690.

Hallett, R. B. & Kyle, P. R. (1993). XRF and INAA determinations of major and trace elements in Geological Survey of Japan igneous and sedimentary rock standards. *Geostandards Newsletter* **17**, 127–133.

Handler, M. R., Wysoczanski, R. J. & Gamble, J. A. (2003). Proterozoic lithosphere in Marie Byrd Land, West Antarctica: Re–Os systematics of spinel peridotite xenoliths. *Chemical Geology* **196**, 131–145.

Hart, S. R. & Davis, K. E. (1978). Nickel partitioning between olivine and silicate melt. *Earth and Planetary Science Letters* **40**, 203–219.

Hart, S. R. & Dunn, T. (1993). Experimental Cpx/melt partitioning of 24 trace-elements. *Contributions to Mineralogy and Petrology* **113**, 1–8.

Hart, S. R. & Kyle, P. R. (1994). Geochemistry of McMurdo Group volcanic rocks. *Antarctic Journal of the United States* **28**, 14–16.

Hart, S. R., Hauri, E. H., Oschmann, L. A. & Whitehead, J. A. (1992). Mantle plumes and entrainment: isotopic evidence: *Science* **256**, 517–520.

Hart, S. R., Blusztajn, J. & Craddock, C. (1995). Cenozoic volcanism in Antarctica; Jones Mountains and Peter I Island. *Geochimica et Cosmochimica Acta* **59**, 3379–3388.

Hart, S. R., Blusztajn, J., LeMasurier, W. E. & Rex, D. C. (1997). Hobbs Coast Cenozoic volcanism: implications for the West Antarctic rift system. *Chemical Geology* **139**, 223–248.

Hart, S. R., Gaetani, G. A. & Kelemen, P. B. (2005). Mantle Pb paradoxes: the sulfide solution. *EOS Transactions, American Geophysical Union* **86**(52), Fall Meeting Supplement, Abstract V23D-06.

Hauri, E. H. & Hart, S. R. (1993). Re–Os isotope systematics of HIMU and EMII oceanic island basalts from the South Pacific Ocean. *Earth and Planetary Science Letters* **114**, 353–371.

Hauri, E. H., Wagner, T. P. & Grove, T. L. (1994). Experimental and natural partitioning of Th, U, Pb and other trace elements between garnet, clinopyroxene and basaltic melts. *Chemical Geology* **117**, 149–166.

Hawkesworth, C. J., Gallagher, K., Hergt, J. M. & McDermott, F. (1993). Trace element fractionation processes in the generation of island arc basalts. *Philosophical Transactions of the Royal Society of London* **342**, 179–191.

Hergt, J. M. & Brauns, C. M. (2001). On the origin of Tasmanian dolerites. *Australian Journal of Earth Sciences* **48**, 543–549.

Hergt, J. M., Peate, D. W. & Hawkesworth, C. J. (1991). The petrogenesis of Mesozoic Gondwana low-Ti flood basalts. *Earth and Planetary Science Letters* **105**, 134–148.

Herzberg, C. & Zhang, J. (1996). Melting experiments on anhydrous peridotite KLB-1: compositions of magmas in the upper mantle and transition zone. *Journal of Geophysical Research* **101**, 8271–8295.

Hirose, K. & Kushiro, I. (1993). Partial melting of dry peridotites at high pressures; determination of compositions of melts segregated from peridotite using aggregates of diamond. *Earth and Planetary Science Letters* **114**, 477–489.

Hofmann, A. W. (1997). Mantle geochemistry: a message from oceanic volcanism. *Nature* **385**, 219–229.

Hofmann, A. W., Jochum, K. P., Seufert, M. & White, W. M. (1986). Nb and Pb in oceanic basalts: new constraints on mantle evolution. *Earth and Planetary Science Letters* **79**, 33–45.

Hoke, L., Poreda, R., Reay, A. & Weaver, S. D. (2000). The subcontinental mantle beneath southern New Zealand, characterized by helium isotopes in intraplate basalts and gas-rich springs. *Geochimica et Cosmochimica Acta* **64**, 2489–2507.

Hole, M. J. & LeMasurier, W. E. (1994). Tectonic controls on the geochemical composition of Cenozoic, mafic alkaline volcanic rocks from West Antarctica. *Contributions to Mineralogy and Petrology* **117**, 187–202.

Hole, M. J., Kempton, P. D. & Miller, I. L. (1993). Trace-element and isotopic characteristics of small-degree melts of the asthenosphere: evidence from the alkalic basalts of the Antarctic Peninsula. *Chemical Geology* **109**, 51–68.

Huang, Y., Hawkesworth, C., van Calsteren, P., Smith, I. & Black, P. (1997). Melt generation models for the Auckland volcanic field, New Zealand: constraints from U–Th isotopes. *Earth and Planetary Science Letters* **149**, 67–84.

Ionov, D. A. & A. W. Hofmann (1995). Nb–Ta-rich mantle amphiboles and micas: implications for subduction-related metasomatic trace element fractionations. *Earth and Planetary Science Letters* **131**, 341–356.

Ionov, D. A., Grégoire, M. & Prikhod'ko, V. S. (1999). Feldspar–Ti-oxide metasomatism in off-cratonic continental and oceanic upper mantle. *Earth and Planetary Science Letters* **165**, 37–44.

Janney, P. E., Le Roex, A. P., Carlson, R. W. & Viljoen, K. S. (2002). A chemical and multi-isotope study of the Western Cape olivine melilitite province, South Africa: implications for the sources of kimberlites and the origin of the HIMU signature in Africa. *Journal of Petrology* **43**, 2339–2370.

Johnson, R. W. (1989). *Intraplate Volcanism in Eastern Australia and New Zealand*. Cambridge: Cambridge University Press.

Kamenetsky, V. S., Everard, J. L., Crawford, A. J., Varne, R., Eggins, S. M. & Lanyon, R. (2000). Enriched end-member of primitive MORB melts: petrology and geochemistry of glasses from Macquarie Island (SW Pacific). *Journal of Petrology* **41**, 411–430.

Keppler, H. (1996). Constraints from partitioning experiments on the composition of subduction-zone fluids. *Nature* **380**, 237–240.

King, S. D. & Anderson, D. L. (1995). An alternative mechanism of flood basalt formation. *Earth and Planetary Science Letters* **136**, 269–279.

Kyle, P. R., Pankhurst, R. J. & Bowman, J. R. (1983). Isotopic and chemical variations in Kirkpatrick Basalt Group rocks from South Victoria Land. In: Oliver, R. L., James, P. R. & Jago, J. B. (eds) *Antarctica Earth Sciences*. Canberra, ACT: Australian Academy of Science, pp. 234–237.

Laird, M. G. (1993). Cretaceous continental rifts: New Zealand region. In: Ballance, P. F. (ed.) *South Pacific Sedimentary Basins. Sedimentary Basins of the World, 2*. Amsterdam: Elsevier, pp. 37–49.

Laird, M. G. & Bradshaw, J. D. (2004). The break-up of a long-term relationship: the Cretaceous separation of New Zealand from Gondwana. *Gondwana Research* **7**, 273–286.

Lanyon, R., Varne, R. & Crawford, A. J. (1993). Tasmanian Tertiary basalts, the Balleny plume, and opening of the Tasman Sea (southwest Pacific Ocean). *Geology* **21**, 555–558.

Larter, R. D., Cunningham, A. P., Barker, P. F., Gohl, K. & Nitsche, F. O. (2002). Tectonic evolution of the Pacific margin of Antarctica: 1. Late Cretaceous tectonic reconstructions. *Journal of Geophysical Research* **107** (B12), 2345, doi:10.1029/2000JB000052.

LaTourrette, T., Hervig, R. L. & Holloway, J. R. (1995). Trace element partitioning between amphibole, phlogopite, and basanite melt. *Earth and Planetary Science Letters* **135**, 13–30.

Lawver, L. A., Gahagan, L. M. & Coffin, M. F. (1992). The development of paleoseaways around Antarctica: the Antarctic paleoenviornment: a perspective on global change. *Antarctic Research Series, American Geophysical Union* **56**, 7–30.

Le Maitre, R. W. (2002). *Igneous Rocks: A Classification and Glossary of Terms*. Cambridge: Cambridge University Press, 236 pp.

LeMasurier, W. E. & Landis, C. A. (1996). Mantle-plume activity recorded by low-relief erosion surfaces in West Antarctica and New Zealand. *Geological Society of America Bulletin* **108**, 1450–1466.

LeMasurier, W. E. & Rex, D. C. (1989). Evolution of linear volcanic ranges in Marie Byrd Land, West Antarctica. *Journal of Geophysical Research* **94**, 7223–7236.

Lloyd, F. E. & Bailey, D. K. (1975). Light element metasomatism of the continental mantle: the evidence and the consequences. *Physics and Chemistry of the Earth* **9**, 389–416.

Luyendyk, B. P. (1995). Hypothesis for Cretaceous rifting of east Gondwana caused by subduction slab capture. *Geology* **23**, 373–376.

Luyendyk, B. P., Sorlien, C. C., Wilson, D. S., Bartek, L. R. & Siddoway, C. S. (2001). Structural and tectonic evolution of the Ross Sea rift in the Cape Colbeck region, Eastern Ross Sea, Antarctica. *Tectonics* **20**, 933–958.

Luyendyk, B. P., Wilson, D. & Siddoway, C. (2003). Eastern margin of the Ross Sea Rift in western Marie Byrd Land, Antarctica: crustal structure and tectonic development, *Geochemistry, Geophysics, Geosystems*, **4** (10), 1090, doi:10.1029/2002GC000462.

McDonough, W. F. & Sun, S. S. (1995). The composition of the Earth. In: McDonough, W. F., Arndt, N. T. & Shirey, S. (eds) *Chemical Geology*. Amsterdam: Elsevier, pp. 223–253.

McKenzie, D. & Bickle, M. J. (1988). The volume and composition of melt generated by extension of the lithosphere. *Journal of Petrology* **29** (3), 625–679.

Mengel, K. & Green, D. H. (1986). Stability of amphibole and phlogopite in metasomatized peridotite under water-saturated and water-undersaturated conditions. In: Ross, J., Jaques, A. L., Ferguson, J., Green, D. H., O'Reilly, S. Y., Danchin, R. V. & Janse, A. J. A. (eds) *Kimberlites and Related Rocks*. Oxford: Blackwell Science, pp. 571–581.

Molnar, P., Atwater, T., Mammerickx, J. & Smith, S. M. (1975). Magnetic anomalies, bathymetry and the tectonic evolution of the South Pacific since the Late Cretaceous. *Geophysical Journal of the Royal Astronomical Society* **40**, 383–420.

Molzahn, M., Reisberg, L. & Wörner, G. (1996). Os, Sr, Nd, Pb, O isotope and trace element data from the Ferrar flood basalts, Antarctica: evidence for an enriched subcontinental lithosphere source. *Earth and Planetary Science Letters* **144**, 529–546.

Moreira, M. & Kurz, M. D. (1999). Subducted oceanic lithosphere and the origin of the 'high μ' basalt helium isotopic signature. *Earth and Planetary Science Letters* **189**, 49–57.

Morris, P. A. (1984). Petrology of the Campbell Island volcanics, southwest Pacific Ocean. *Journal of Volcanology and Geothermal Research* **21**, 119–148.

Morris, P. A. (1985*a*). Petrology of Late Cretaceous alkaline volcanic rocks from the Chatham Islands, New Zealand. *New Zealand Journal of Geology and Geophysics* **28**, 253–266.

Morris, P. A. (1985*b*). The geochemistry of Eocene–Oligocene volcanics on the Chatham Islands, New Zealand. *New Zealand Journal of Geology and Geophysics* **28**, 459–469.

Morris, P. A. & Gamble, J. A. (1990). Campbell Island. In: LeMasurier, W. E. & Thomson, J. W. (eds) *Volcanoes of the Antarctic Plate and Southern Oceans. Antarctic Research Series, American Geophysical Union* **48**, 474–475.

Mortimer, N. & Roser, B. P. (1992). Geochemical evidence for the position of the Caples–Torlesse boundary in the Otago Schist, New Zealand. *Journal of the Geological Society, London* **149**, 967–977.

Mukasa, S. B. & Dalziel, I. W. D. (2000). Marie Byrd Land, West Antarctica: evolution of Gondwana's Pacific margin constrained by zircon U–Pb geochronology and feldspar common-Pb isotopic compositions. *Geological Society of America Bulletin* **112**, 611–627.

Müller, R. D., Royer, J.-Y. & Lawver, L. A. (1993). Revised plate motions relative to the hotspots from combined Atlantic and Indian Ocean hotspot tracks. *Geology* **21**, 275–278.

Navon, O. & Stolper, E. (1987). Geochemical consequences of melt percolation: the upper mantle as a chromatographic column. *Journal of Geology* **95**, 285–307.

Niida, K. & Green, D. H. (1999). Stability and chemical composition of pargasitic amphibole in MORB pyrolite under upper mantle conditions. *Contributions to Mineralogy and Petrology* **135**, 18–40.

Orlando, A., Conticelli, S., Armienti, P. & Borrini, D. (2000). Experimental study on a basanite from the McMurdo Volcanic Group, Antarctica; inference on its mantle source. *Antarctic Science* **12** (1), 105–116.

Pankhurst, R. J., Weaver, S. D., Bradshaw, J. D., Storey, B. C. & Ireland, T. R. (1998). Geochronology and geochemistry of pre-Jurassic superterranes in Marie Byrd Land, Antarctica. *Journal of Geophysical Research* **103**, 2529–2547.

Panter, K. S., Kyle, P. R. & Smellie, J. L. (1997). Petrogenesis of a phonolite–trachyte succession at Mount Sidley, Marie Byrd Land, Antarctica. *Journal of Petrology* **38**, 1225–1253.

Panter, K. S., Hart, S. R., Kyle, P., Blusztanjn, J. & Wilch, T. (2000*a*). Geochemistry of Late Cenozoic basalts form the Crary Mountains: characterization of mantle sources in Marie Byrd Land, Antarctica. *Chemical Geology* **165**, 215–241.

Panter, K. S., Hart, S. R. & Kyle, P. (2000*b*). Evidence for a Cretaceous Antarctic plume ('Erebus Plume') in New Zealand. *EOS Transactions, American Geophysical Union* **81**, F1357.

Panter, K. S., Blusztajn, J., Wingrove, D., Hart, S. & Mattey, D. (2003). Sr, Nd, Pb, Os, O isotope, major and trace element data from basalts, South Victoria Land, Antarctica: evidence for open-system processes in the evolution of mafic alkaline magmas: *European Geophysical Society, Geophysical Research Abstracts* **5**, 07583.

Pilet, S., Hernandez, J., Sylvester, P. J. & Poujol (2005). The metasomatic alternative for ocean island basalt chemical heterogeneity. *Earth and Planetary Science Letters* **236**, 148–166.

Price, R. C., Cooper, A. F., Woodhead, J. D. & Cartwright, I. (2003). Phonolite diatremes within the Dunedin Volcano, South Island, New Zealand. *Journal of Petrology* **44** (11), 2053–2080.

Richard, S. M., Smith, C. H., Kimbrough, D. L., Fitzgerald, P. G., Luyendyk, B. P. & McWilliams, M. O. (1994). Cooling history of the northern Ford Ranges, Marie Byrd Land, West Antarctica. *Tectonics* **13**, 837–857.

Rocchi, S., Armienti, P., D'Orazio, M., Tonarini, S., Wijbrans, J. R. & Di Vincenzo, G. (2002). Cenozoic magmatism in the western Ross Embayment: role of mantle plume versus plate dynamics in the development of the West Antarctic Rift System. *Journal of Geophysical Research* **107** (B9), 2195.

Rocchi, S., Armienti, P. & Di Vincenzo, G. (2004). No plume, no rift magmatism in the west Antarctic rift. In: Foulger, G. R., Anderson, D. L., Natland, J. H. & Presnall, D. C. (eds) *Plates, Plumes and Paradigms. Geological Society of America, Special Papers* **388**, 435–447.

Rocholl, A., Stein, M., Molzahn, M., Hart, S. R. & Wörner, G. (1995). Geochemical evolution of rift magmas by progressive tapping of a stratified mantle source beneath the Ross Sea rift, northern Victoria Land, Antarctica. *Earth and Planetary Science Letters* **131**, 207–224.

Rudnick, R. L & Fountain, D. M. (1995). Nature and composition of the continental crust; a lower crustal perspective. *Reviews of Geophysics* **33**, 267–309.

Salters, V. J. M., Longhi, J. E. & Bizimis, M. (2002). Near mantle solidus trace element partitioning at pressures up to 3·4 GPa. *Geochemistry, Geophysics and Geosystems* **3** (7), doi:10.1029/2001GC000148.

Scherwath, M., Stern, T. & Molnar, P. (2002). Pn anisotropy and distributed upper mantle deformation associated with a continental transform fault. *Geophysical Research Letters* **29**, 1175, doi:10.1029/2001GL014179.

Schmidt, K. H., Bottazzi, P., Vannucci, R. & Mengel, K. (1999). Trace element partitioning between phlogopite, clinopyroxene and leucite lamproite melt. *Earth and Planetary Science Letters* **168**, 287–299.

Simons, F. J., Zielhuis, A. & van der Hilst, R. D. (1999). The deep structure of the Australian continent from surface wave tomography. *Lithos* **48**, 17–43.

Simons, F. J., van der Hilst, R. D. & Zuber, M. T. (2003). Spatiospectral localization of isostatic coherence anisotropy in Australia and its relation to seismic anisotropy: implications for lithospheric deformation. *Journal of Geophysical Research* **108**, 2250, doi:10.1029/2001JB000704.

Sims, K. W. W. & DePaolo, D. J. (1997). Inferences about mantle magma sources from incompatible element concentration ratios in oceanic basalts. *Geochimica et Cosmochimica Acta* **61**, 765–784.

Späth, A., Le Roex, A. P. & Opiyo-Akech, N. (2001). Plume–lithosphere interaction and the origin of continental rift-related alklaline volcanism—the Chyulu Hills volcanic province, southern Kenya. *Journal of Petrology* **42**, 765–787.

Spell, T. L., McDougall, I. & Tulloch, A. J. (2000). Thermochronologic constraints on the breakup of the Pacific Gondwana margin: the Paparoa metamorphic core complex, South Island, New Zealand. *Tectonics* **19**, 433–451.

Steiger, R. H. & Jäger, E. (1977). Subcommission on geochronology: convention on the use of decay constants in geo- and cosmochronology. *Earth and Planetary Science Letters* **36**, 359–362.

Stein, M & Hofmann, A. W. (1992). Fossil plume head beneath the Arabian lithosphere? *Earth and Planetary Science Letters* **114**, 193–209.

Stein, M., Navon, O. & Kessel, R. (1997). Chromatographic metasomatism of the Arabian–Nubian lithosphere. *Earth and Planetary Science Letters* **152**, 75–91.

Storey, B. C. (1995). The role of mantle plumes in continental breakup: case histories from Gondwanaland. *Nature* **377**, 301–308.

Storey, B. C. & Kyle, P. R. (1997). An active mantle mechanism for Gondwana breakup. *South African Journal of Geology* **100** (4), 283–290.

Storey, B. C., Leat, P. T., Weaver, S. D., Pankhurst, R. J., Bradshaw, J. D. & Kelly, S. (1999). Mantle plumes and Antarctica–New Zealand rifting: evidence from mid-Cretaceous mafic dykes. *Journal of the Geological Society, London* **156**, 659–671.

Storey B. C., Leat, P. T. & Ferris, J. K. (2001). The location of mantle-plume centers during the initial stages of Gondwana breakup. In: Ernst, R. E. & Buchan, K. L. (eds) *Mantle Plumes: Their Identification Through Time. Geological Society of America, Special Papers* **352**, 71–80.

Stracke, A., Bizimis, M. & Salters, V. J. M. (2003). Recycling oceanic crust: quantitative constraints. *Geochemistry, Geophysics, Geosystems* **4** (3), 8003, doi:10.1029/2001GC000223.

Stracke, A., Hofmann, A. W. & Hart, S. R. (2005). FOZO, HIMU, and the rest of the mantle zoo. *Geochemistry, Geophysics, Geosystems* **6** (5), 5007, doi:10·1029/2004GC000824.

Sun, S.-S. & Hanson, G. N. (1975). Rare earth element evidence for differentiation of McMurdo Volcanics, Ross Island, Antarctica. *Contributions to Mineralogy and Petrology* **54**, 139–155.

Sun, S.-S., McDonough, W. F. & Ewart, A. (1989). Four component model for East Australian Basalts. In: Johnson, R. W. (ed.) *Intraplate Volcanism in Eastern Australia and New Zealand*. Cambridge: Cambridge University Press, pp. 333–347.

Sutherland, R. (1995). The Australia–Pacific boundary and Cenozoic plate motions in the SW Pacific: some constraints from Geosat data. *Tectonics* **14**, 819–831.

Sutherland, R. (1999). Basement geology and tectonic development of the greater New Zealand region: an interpretation from regional magnetic data. *Tectonophysics* **308**, 341–362.

Tiepolo, M., Vannucci, R., Oberti, R., Foley, S., Bottazzi, P. & Zanetti, A. (2000). Nb and Ta incorporation and fractionation in titanian pargasite and kaersutite: crystal-chemical constraints and implications for natural systems. *Earth and Planetary Science Letters* **176**, 185–201.

Todt, W., Cliff, R. A., Hanser, A. & Hofmann, A. W. (1996). Evaluation of a ^{202}Pb–^{205}Pb double spike for high-precision lead isotope analysis. In: Basu, A. & Hart, S. R. (eds) *Earth Processes: Reading the Isotopic Code. Geophysical Monograph, American Geophysical Union* **95**, 429–437.

Trønnes, R. G. (2002). Stability range and decomposition of potassic richterite and phlogopite end members at 5–15 GPa. *Mineralogy and Petrology* **74**, 129–148.

Tulloch, A. J. & Kimbrough, D. L. (1989). The Paparoa metamorphic core complex, New Zealand: Cretaceous extension associated with fragmentation of the Pacific margin of Gondwana. *Tectonics* **8**, 1217–1234.

Tulloch, A. J. & Kimbrough, D. L. (1995). Mesozoic plutonism in western New Zealand—a 50 Ma transition from subduction to continental rifting on the Gondwana margin. In: Brown, M. & Piccoli, P. (eds) *The Origin of Granites and Related Rocks. Third Hutton Symposium, Abstracts. US Geological Survey Circular* **1129**, 153–156.

van Achterbergh, E., Griffin, W. L. & Stiefenhofer, J. (2001). Metasomatism in mantle xenoliths from the Letlhakane kimberlites:

estimation of element fluxes. *Contributions to Mineralology and Petrology* **141**, 397–414.

van Westrenen, W., Blundy, J. B. & Wood, B. J. (2001). High field strength element/rare earth element fractionation during partial melting in the presence of garnet: implications for identification of mantle heterogeneities. *Geochemistry, Geophysics, Geosystems* **2**, paper number 2000GC000133.

Vlastélic, I., Aslanian, D., Dosso, L., Bougault, H., Olivet, J. L. & Géli, L. (1999). Large-scale chemical and thermal division of the Pacific mantle. *Nature* **399**, 345–350.

Waight, T. E., Weaver, S. D. & Muir, R. J. (1998*a*). Mid-Cretaceous granitic magmatism during the transition from subduction to extension in southern New Zealand: a chemical and tectonic synthesis. *Lithos* **45**, 469–482.

Waight, T. E., Eby, G. N., Maas, R. & Weaver, S. D. (1998*b*). French Creek Granite and Hohonu dyke swarm, South Island, New Zealand; Late Cretaceous alkaline magmatism and the opening of the Tasman Sea. *Australian Journal of Earth Sciences* **45** (6), 823–835.

Walcott, R. I. (1998). Modes of oblique compression: late Cenozoic tectonics of the South Island of New Zealand. *Reviews of Geophysics* **36**, 1–26.

Wass, S. Y. & Rogers, N. W. (1980). Mantle metasomatism: precursor to continental alkaline volcanism. *Geochimica et Cosmochimica Acta* **44**, 1811–1823.

Watters, W. A., Campbell, H. J. & Adams, C. J. D. (1987). Notes on the geology of Southeast Island and Star Keys, Chatham Islands. *New Zealand Geological Survey Record* **20**, 139–145.

Weaver, S. D. & Pankhurst, R. J. (1991). A precise Rb–Sr age for the Mandamus igneous complex, North Canterbury, and regional tectonic implications. *New Zealand Journal of Geology and Geophysics* **34**, 341–345.

Weaver, S. D. & Smith, I. E. M. (1989). New Zealand intraplate volcanism. In: Johnson, R. W., Knutson, J. & Taylor, S. R. (eds) *Intraplate Volcanism in Eastern Australia and New Zealand*. Cambridge: Cambridge University Press; Canberra, ACT: Australian Academy of Science, pp. 157–187.

Weaver, S. D., Storey, B. C., Pankhurst, R. J., Mukasa, S. B., DiVenere, V. J. & Bradshaw, J. D. (1994). Antarctica–New Zealand rifting and Marie Byrd Land lithospheric magmatism linked to ridge subduction and mantle plume activity. *Geology* **22**, 811–814.

Willis, M. J., Wilson, T. J. & James, T. S. (2004). Neotectonic crustal motions in the Antarctic interior measured by the TAMDEF GPS network. *EOS Transactions, American Geophysical Union* **85** (17), JA123.

Wilson, M., Rosenbaum, J. M. & Dunworth, E. A. (1995). Melilitites: partial melts of the thermal boundary layer? *Contributions to Mineralogy and Petrology* **119**, 181–196.

Winberry, J. P. & Anandakrishnan, S. (2003). Seismicity and neotectonics of West Antarctica. *Geophysical Research Letters* **30,** SDE 1–4.

Wood, R. A. & Herzer, R. H. (1993). The Chatham Rise, New Zealand. In: Ballance, P. F. (ed.) *South Pacific Sedimentary Basins. Sedimentary Basins of the World, 2*. Amsterdam: Elsevier, pp. 329–348.

Workman, R. K., Hart, S. R., Jackson, M., Regelous, M., Farley, K. A., Blusztajn, J., Kurz, M. & Staudigel, H. (2004). Recycled metasomatized lithosphere as the origin of the Enriched Mantle II (EM2) end-member: evidence from the Samoan volcanic chain. *Geochemistry, Geophysics, Geosystems* **5** (4), Q04008, doi:10.1029/2003GC000623.

Zanetti, A., Vannucci, R., Bottazzi, P., Oberti, R. & Ottolini, L. (1996). Infiltration metasomatism at Lherz as monitored by systematic ion-microprobe investigations close to a hornblendite vein. *Chemical Geology* **134**, 113–133.

Zhang, M. & O'Reilly, S. Y. (1997). Multiple sources for basaltic rocks from Dubbo, eastern Australia: geochemical evidence for plume–lithosphere mantle interaction. *Chemical Geology* **136**, 33–54.

Zhang, M., O'Reilly, S. Y. & Chen, D. (1999). Location of Pacific and Indian mid-ocean ridge-type mantle in two time slices: evidence from Pb, Sr, and Nd isotopes for Cenozoic Australian basalts. *Geology* **27**, 39–42.

Zindler, A. & Hart, S. R. (1986). Chemical geodynamics. *Annual Review of Earth and Planetary Sciences* **14**, 493–571.